INT. J. CONTROL, 2004, VOL. 77, NO. 12, 1115–1136

Taylor & Francis
Taylor & Francis Group

Robust stabilization of infinite-dimensional systems using sliding-mode output feedback control

YURY ORLOV†, YIMING LOU‡ and PANAGIOTIS D. CHRISTOFIDES‡*

Sliding mode based feedback control has long been recognized as a powerful, yet easy-to-implement, control method to counteract non-vanishing external disturbances and unmodelled dynamics. Recently, research attention has focused on the development of sliding mode feedback control methods for various classes of infinite-dimensional systems. However, the existing methods are based on the assumption that distributed sensing and actuation is available, which significantly restricts their applicability to distributed process control applications. In this work, a sliding mode output feedback control method is developed for a class of linear infinite-dimensional systems with finite-dimensional unstable part using finite-dimensional sensing and actuation. Modal decomposition is initially used to decompose the original infinite-dimensional system into an interconnection of a finite-dimensional (possibly unstable) system and an infinite-dimensional stable system. Then, a sliding mode-based stabilizing state feedback controller is constructed on the basis of the finite-dimensional system. Subsequently, an infinite-dimensional Luenberger state observer, which utilizes a finite number of measurements, is constructed to provide estimates of the state of the infinite-dimensional system. Finally, an output feedback controller design is completed by coupling the infinite-dimensional Luenberger state observer and the sliding mode-based state feedback controller. Implementation, performance and robustness issues of the sliding-mode output feedback controller are illustrated in a simulation study of a distributed parameter system governed by the linearization around the spatially-uniform steady-state solution of the Kuramoto–Sivashinsky partial differential equation with periodic boundary conditions.

1. Introduction

Sliding-mode control has long been recognized as a powerful control method to counteract non-vanishing external disturbances and unmodelled dynamics (Utkin 1992). This method is based on the deliberate introduction of sliding motions into the control system and consists of two steps. First, a manifold is designed such that if confined to this manifold the system has desired dynamic properties. Second, a switched control law, which drives the system to the manifold, is synthesized. The controller, thus constructed, asymptotically stabilizes the system and since the motion along the manifold proves to be uncorrupted by matched disturbances, the closed-loop system is additionally guaranteed to have strong robustness properties against matched disturbances. Due to these advantages and simplicity of implementation, sliding-mode controllers have widely been used in various applications (Utkin *et al.* 1999).

Motivated by technological advances, significant interest has emerged in extending this discontinuous control method to distributed parameter systems (DPS). The earlier works (Orlov and Utkin 1987, Zolezzi 1989) on extensions of discontinuous control algorithms to infinite-dimensional systems ran into a major difficulty, caused by the presence of an unbounded infinitesimal operator in the plant equation, and called for further theoretical investigations. Presently, the discontinuous control synthesis in the infinite-dimensional setting is well documented (Orlov 2000, Levaggi 2002 a,b, Orlov and Dochain 2002). This synthesis retains robustness features, similar to those possessed by its counterpart in the finite-dimensional case. Being complementary to the H_∞-design (van Keulen 1993, Curtain and Zwart 1995, Foias *et al.* 1996) it constitutes an alternative approach to control of infinite-dimensional systems.

However, the existing results on discontinuous control of infinite-dimensional systems are based on the assumption that distributed sensing and actuation is available over the entire spatial domain. Although due to recent advances in micro-electro-mechanical-systems (MEMS) technology, manufacturing large arrays of micro sensors and actuators with integrated control circuitry has become feasible (see (Ho and Tai 1998) and references quoted therein), implementation of distributed sensors and actuators is hardly possible in many real-life applications where the available number of sensors and actuators is typically small. Thus, the development of discontinuous control methods for infinite-dimensional systems with finite-dimensional sensing and actuation is a fundamental problem of relevance to various practical applications.

In this work, an output feedback control method based on sliding modes is developed for a class of linear infinite-dimensional systems with finite-dimensional unstable part using finite-dimensional sensing and actuation. For these systems, our main results include: (1) the discontinuous output feedback controller

Received 25 June 2004. Communicated by Professor V. Utkin.

*Author for correspondence. e-mail: pdc@seas.ucla.edu

†CICESE Research Center, Electronics and Telecommunication Department, P.O. Box 434944 San Diego, CA 92143-4944, USA.

‡Department of Chemical Engineering, University of California, Los Angeles, CA 90095, USA.

International Journal of Control ISSN 0020–7179 print/ISSN 1366–5820 online © 2004 Taylor & Francis Ltd
http://www.tandf.co.uk/journals
DOI: 10.1080/00207170420002730 78

synthesis based on sliding modes in the infinite-dimensional setting, and (2) the justification of the implementation of the discontinuous sliding-mode controller via its continuous approximation.

Initially, the class of infinite-dimensional system is precisely formulated. Modal decomposition is then used to decompose the original infinite-dimensional system into an interconnection of a finite-dimensional (possibly unstable) system and an infinite-dimensional stable system. A sliding mode-based stabilizing state feedback controller is constructed on the basis of the finite-dimensional system. Subsequently, an infinite-dimensional Luenberger state observer, which utilizes a finite-number of measurements, is constructed to provide estimates of the state of the infinite-dimensional system. Finally, an output feedback controller design is completed by coupling the infinite-dimensional Luenberger state observer and the sliding mode-based state feedback controller. In order to obtain the fully practical finite-dimensional framework for controller synthesis, a finite-dimensional approximation of the Luenberger observer as well as a continuous approximation of the sliding-mode controller are carried out at the implementation stage.

Implementation, performance and robustness issues of the sliding-mode output feedback control design are illustrated in a simulation study of a distributed parameter system governed by the linearization of the Kuramoto–Sivashinsky equation around the spatially-uniform steady-state solution with periodic boundary conditions. While being unforced, the KSE describes incipient instabilities in a variety of physical and chemical systems and a control problem that occurs here is to avoid the appearance of the instabilities in the closed-loop system (Christofides and Armaou 2000) (see also Christofides (2001) for other results on control of PDE systems). We also note several recent works on control of the Kuramoto–Sivashinsky equation including boundary control (Liu and Krstić 2001) as well as methods for robust (Hu and Temam 2001) and adaptive (Kobayashi 2002) stabilization.

The outline of the paper is as follows. Background material on infinite-dimensional systems is given in § 2. Sliding-mode output feedback controller synthesis, augmented with a proper continuous approximation, is developed in § 3. Numerical results appear in § 4. Finally, § 5 presents some conclusions.

2. Preliminaries

We consider infinite-dimensional systems, defined in a Hilbert space H, of the form:

$$\dot{x} = Ax + Bu \tag{1}$$

$$y = Cx \tag{2}$$

where $x \in H$ is the state, $u \in R^m$ is the control input, $y \in R^p$ is the measured output, A is an infinitesimal operator which generates a C_0 (strongly continuous) semigroup $T_A(t)$, $B \in \mathcal{L}(R^m, H)$ and $C \in \mathcal{L}(H, R^p)$. Hereinafter, the notation is fairly standard. Particularly, given Hilbert spaces U and H, the symbol $\mathcal{L}(U, H)$ stands for the set of linear bounded operators from U to H. All relevant background material on infinite-dimensional dynamic systems in a Hilbert space can be found, e.g. in Curtain and Zwart (1995).

Given an initial condition

$$x(0) = x^0 \in H \tag{3}$$

it is well-known that the Hilbert space-valued differential equation (1) with a continuously differentiable control input $u(x)$ has a unique local mild solution $x(t)$ (Pazy 1983). By default, only mild solutions are under study in the present work. The precise meaning of the solution of (**1**), for inputs which are only piecewise continuously differentiable, is defined as a limiting result obtained through the following regularization procedure.

Let the control input $u(x)$ undergo discontinuities on the hyperplane

$$\sigma x = 0, \quad \sigma \in \mathcal{L}(H, R^m) \tag{4}$$

and let $u(x)$ be continuously differentiable beyond this hyperplane. Then the trajectories of (1) are defined in the conventional sense whenever they are beyond the discontinuity hyperplane (4) whereas in a vicinity of this hyperplane the original system is replaced by a related system, which takes into account all possible imperfections in the new control input $u^\delta(x)$ (e.g. delay, hysteresis, saturation, etc.) and for which there exists a conventional solution. A motion along the discontinuity hyperplane, if any, is then obtained by making the characteristics of the new system approach those of the original one. Such a motion is further referred to as a sliding mode that has become standard in the literature. The rigorous introduction of the solution concept is as follows (Orlov and Dochain 2002).

Definition 1: An absolutely continuous function $x^\delta(t)$, defined on some interval $[0, \tau)$, is said to be an approximate δ-solution of system (1) if it is a conventional solution of

$$\dot{x}^\delta = Ax^\delta + Bu^\delta(x^\delta)$$

with some $u^\delta(x)$ such that

$$\|u^\delta(x) - u(x)\| \leq \delta \quad \text{for all} \quad x \in H \text{ subject to } \|\sigma x\| \geq \delta. \tag{5}$$

Definition 2: An absolutely continuous function $x(t)$, defined on some interval $[0, \tau)$, is said to be a solution of system (1) if there exists a family of δ-solutions $x^\delta(t)$ of the system such that

$$\lim_{\delta\to 0}\|x^\delta(t)-x(t)\|=0 \quad \text{uniformly in} \quad t\in[0,\tau).$$

Thus, by definition the sliding motion, which is in general non-unique, does not depend on the precise specification of the discontinuous input on the discontinuity hyperplane. Moreover, an equivalent control value $u_{\mathrm{eq}}(x)$, maintaining the system motion on this hyperplane, is imposed by the original system itself. If the $m\times m$-matrix (σB) is non-singular there exists a unique solution of the equation $\sigma\dot{x}=0$, i.e. $\sigma Ax+\sigma Bu=0$ with respect to u and this solution

$$u_{\mathrm{eq}}(x)=-(\sigma B)^{-1}\sigma Ax \tag{6}$$

is accepted as the equivalent control value because (6) is the only controller maintaining system (1) with appropriate initial conditions on the hyperplane $\sigma x=0$. According to the infinite-dimensional extension (Orlov 2000, Orlov and Dochain 2002) of the equivalent control method (Utkin 1992), the so-called sliding mode equation

$$\dot{x}=[A-B(\sigma B)^{-1}\sigma A]x \tag{7}$$

governing the system motion on the discontinuity hyperplane $\sigma x=0$, is then obtained by substituting the equivalent control value (6) into (1) for u. The following result is extracted from Orlov (2000, Theorem 1).

Theorem 1: *Consider the dynamic system* (1) *subject to the above assumptions and solution formulation. Let* $T(x^0)\geq 0$ *be a finite time, which depends on the initial condition* (3), *in which the system starts evolving in the discontinuity hyperplane* (4) *and let the operator* $\tilde{A}=A-B(\sigma B)^{-1}\sigma A$ *generate an exponentially stable semigroup. Then the initial value problem* (1), (3) *has a unique solution, and this solution is governed by the sliding mode equation* (7) *for* $t\geq T(x^0)$.

For convenience of the reader, we recall the definition of the generator of an exponentially stable semigroup as well as that of the exponential stabilizability/detectability (see, e.g. Curtain and Zwart (1995) for details).

Definition 3: The operator $\tilde{A}$ generates an exponentially stable semigroup $\tilde{S}(t)$ iff the initial value problem $\dot{x}=\tilde{A}x$, $x(0)=x^0$ has a unique solution $x(t)=\tilde{S}(t)x^0$, and $\|\tilde{S}(t)\|\leq\omega e^{-\alpha t}$ for all $t\geq 0$ and some positive ω,α.

Definition 4: System (1), (2), or equivalently, the pair $\{A,B\}$ is said to be exponentially stabilizable if there exists $D\in\mathcal{L}(H,R^m)$ such that the operator $A+BD$ generates an exponentially stable semigroup.

Definition 5: System (1), (2), or equivalently, the pair $\{A,C\}$ is said to be exponentially detectable if there exists $L\in\mathcal{L}(R^p,H)$ such that the operator $A+LC$ generates an exponentially stable semigroup.

The following assumption is made throughout.

Assumption 1: *System* (1), (2) *is exponentially stabilizable and detectable.*

Assumption 1 implies that the system (1) and (2) can be exponentially stabilized via linear dynamic output feedback control of the form

$$u(\tilde{x})=D\tilde{x} \tag{8}$$

$$\dot{\tilde{x}}=A\tilde{x}+Bu(\tilde{x})-L(y-C\tilde{x}) \tag{9}$$

where the internal state $\tilde{x}\in H$, and the operators D and L satisfy the condition of the stabilizability/detectability definitions.

Moreover, under the assumption of exponential stabilizability and detectability, H can be decomposed as $H=H_1\oplus H_2$, and the state equation (1) can be rewritten in terms of $x_1\in H_1$ and $x_2\in H_2$, as (Curtain and Zwart 1995, § 5.2)

$$\dot{x}_1=A_1x_1+B_1u \tag{10}$$

$$\dot{x}_2=A_2x_2+B_2u \tag{11}$$

$$y=C_1x_1+C_2x_2 \tag{12}$$

where $H_1=R^n$ is a finite-dimensional subspace, $A_j=A|_{H_j}$, and $C_j=C|_{H_j}$ are the operator restrictions on H_j, $j=1,2$, $B_j=P_jB$ and P_j is the projector on H_j. From Assumption 1, the matrix pairs $\{A_1,B_1\}$ and $\{A_1,C_1\}$ are controllable and observable, respectively, and the operator $A_2=A|_{H_2}$ generates an exponentially stable semigroup $S_{A_2}(t)$ on H_2.

The decomposition (10) and (11) of the original system (1) into a finite-dimensional possibly unstable part (10) and an infinite-dimensional stable part (11) has long been recognized as providing the framework for the design of stabilizing controllers for linear infinite-dimensional systems (see the notes and references quoted in Curtain and Zwart (1995, Chapter 5). Using the decomposition of (10) and (11), the synthesis of dynamic output feedback control laws is obtained as

$$u(\tilde{x}_1)=D_1\tilde{x}_1 \tag{13}$$

$$\dot{\tilde{x}}_1=A_1\tilde{x}_1+B_1u(\tilde{x}_1)-L_1(y-C_1\tilde{x}_1-C_2\tilde{x}_2) \tag{14}$$

$$\dot{\tilde{x}}_2=A_2\tilde{x}_2+B_2u(\tilde{x}_1) \tag{15}$$

where $D_1=D|_{H_1}$, $L_1=P_1L$ are such that the $n\times n$ matrices $A_1+B_1D_1$ and $A_1+L_1C_1$ are Hurwitz. Although the finite-dimensional state estimate $\tilde{x}_1(t)$ is only required in the control law (13), the Luenberger observer design is carried out in the infinite-dimensional setting (14) and (15) to avoid the appearance of the destabilizing spill-over effect in the closed-loop system (see also proof of Theorem 4). The implementation of the above observer can then be performed by obtaining a finite-dimensional approximation of the $\tilde{x}_2$-subsystem of sufficiently high-order.

It is worth noting that there is a body of literature focusing on the construction of the associated Luenberger observers for stabilization of infinite-dimensional systems (see, e.g. Curtain and Zwart (1995, Chapter 5) and references therein). Such a treatment, based on a finite-dimensional approximation of the original infinite-dimensional system, becomes attractive in practice if instabilities due to spill-over effect can be prevented; it additionally ensures strong robustness properties against unmodelled dynamics and parameter variations. In order to enhance performance the approximation-based treatment will subsequently be accompanied by sliding-mode output feedback synthesis, potentially capable of providing this desired robustness feature.

Remark 1: We note that under Assumption 1, the eigenspectrum of the operator A of system (1) could have hyperbolic-like or parabolic-like structure. As an example, in figure 1, we show the eigenspectrum of the linearized Korteweg–de Vries–Burgers (KdVB) equation (left plot), which is a third-order PDE with a hyperbolic-like spectrum and that of the linearized Kuramoto–Sivashinsky equation (KSE) (right plot), which is a fourth-order PDE with a parabolic-like spectrum. Specifically, the linearized KdVB equation takes the form

$$\frac{\partial x}{\partial t} = -\frac{\partial^3 x}{\partial z^3} + a_1 \frac{\partial^2 x}{\partial z^2}$$
$$\frac{\partial^j x}{\partial z^j}(0,t) = \frac{\partial^j x}{\partial z^j}(+\pi,t), \quad j = 0,\dots,2 \tag{16}$$

and the linearized KSE takes the form

$$\frac{\partial x}{\partial t} = -\nu \frac{\partial^4 x}{\partial z^4} - \frac{\partial^2 x}{\partial z^2}$$
$$\frac{\partial^j x}{\partial z^j}(-\pi,t) = \frac{\partial^j x}{\partial z^j}(+\pi,t), \quad j = 0,\dots,3. \tag{17}$$

Both the linearized KdVB and KS partial differential equations belong in the class of linear infinite-dimensional systems considered in this work and satisfy Assumption 1 (see Armaou and Christofides (2000) for results on finite-dimensional control design for the KdVB equation and the KSE).

3. Sliding-mode feedback synthesis

The aim of this section is to demonstrate how the approximation-based approach can be used to globally exponentially stabilize the infinite-dimensional system (1) and (2) by means of discontinuous output feedback control. First, a discontinuous state feedback controller is constructed and then the Luenberger observer (14) and (15) of the unstable modes is involved to synthesize a stabilizing output feedback law.

3.1. *State feedback design*

The stabilizing discontinuous state feedback controller to be developed is based on the deliberate introduction of sliding modes into the finite-dimensional subsystem (10). Taking into account that the infinite-dimensional subsystem (11) is stable and does not require to be stabilized, the discontinuous state feedback, stabilizing subsystem (10), is subsequently shown to simultaneously stabilize the infinite-dimensional closed-loop system (10) and (11). Thus, the discontinuous stabilization of the infinite-dimensional system (10) and (11) is reduced to the sliding-mode finite-dimensional treatment which is as follows (Utkin 1992).

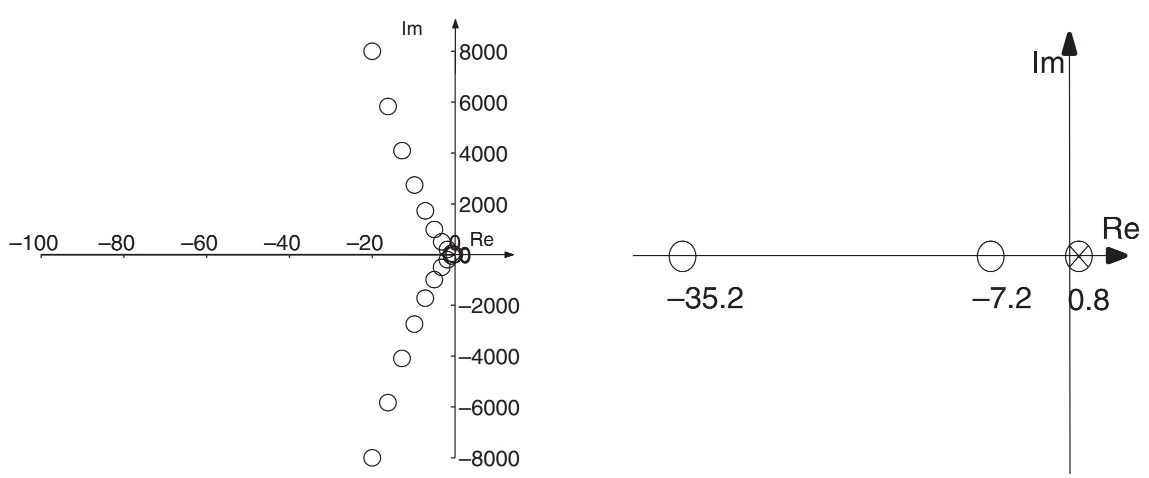

Figure 1. Eigenspectrum of the linearized KdVB equation with $a_1 = 0.05$ (left plot) and that of the linearized KSE with $\nu = 0.2$ (right plot).

The stabilization problem for the finite-dimensional system (10) is solved in the space of the new state variable

$$\xi = Mx_1 \in R^n \tag{18}$$

where $M \in R^{n\times n}$ is a non-singular matrix such that

$$MB_1 = (0, B_{12})^{\mathrm{T}} \tag{19}$$

with a non-singular matrix $B_{12} \in R^{m\times m}$. To satisfy (19), the first $n-m$ rows of M are composed of $n-m$ linearly independent vectors, orthogonal to the control subspace, whereas B_1^{T} forms the remaining m rows of M so that the matrix $B_{12} = B_1^{\mathrm{T}}B_1$ is non-singular.

System (10), rewritten in terms of the components $\xi_1 = P_{11}\xi \in R^{n-m}$, $\xi_2 = P_{12}\xi \in R^m$ of the new state variable $\xi = (\xi_1, \xi_2)^{\mathrm{T}}$, is given by

$$\dot{\xi}_1 = A_{11}\xi_1 + A_{12}\xi_2 \tag{20}$$

$$\dot{\xi}_2 = A_{21}\xi_1 + A_{22}\xi_2 + B_{12}u \tag{21}$$

where P_{11} and P_{12} are the projectors on the subspaces spanned by the first $n-m$ state components and the remaining m components, respectively. By construction, the matrix pair $\{A_1, B_1\}$ is controllable, because the pair $\{A, B\}$, otherwise, would not be exponentially stabilizable. Due to the lemma of Utkin (1992, p. 101), it follows that the matrix pair $\{A_{11}, A_{12}\}$ is also controllable. Then, by an appropriate choice of $K \in R^{m\times(n-m)}$, the matrix $A_{11} + A_{12}K$ can be made Hurwitz with an *a priori* fixed location of the eigenvalues.

The unit signal-based control law can be synthesized in the form

$$u(\xi) = -[\gamma_0 + \gamma_1\|\xi\|]B_{12}^{-1}U(\sigma\xi) \tag{22}$$

with non-negative γ_0

$$\gamma_1 > \|A_{21} - KA_{11}\| + \|A_{22} - KA_{12}\| \tag{23}$$

$$\sigma\xi = \xi_2 - K\xi_1 \tag{24}$$

and

$$U(\sigma\xi) = \frac{\sigma\xi}{\|\sigma\xi\|} \tag{25}$$

to drive the system (20) and (21) to the discontinuity hyperplane $\sigma\xi = 0$. In the above control law, γ_0 and γ_1 are constants, the norm of the unit component $U(\sigma\xi)$ is equal to one everywhere but on the hyperplane $\sigma\xi = 0$, where this component is permitted to be multivalued and take any value from the unit ball $B_1^m = \{u \in R^m\colon \|u\| \le 1\}$.

It should be pointed out that the standard sliding-mode control would also be synthesized to steer the system to the same hyperplane (Utkin 1992). However, this standard approach would result in several switching points as one coordinate after the other hits the hyperplane and in order to design such a controller one would need to additionally follow the hierarchy of the control components that ensures the existence of the sliding motion. In order to simplify the stability analysis and avoid extra computations, required by the hierarchy procedure, the unit feedback controller (22) is synthesized in such a manner that the motion of the closed-loop system never passes through the discontinuity hyperplane. The system stability is thus analyzed beyond the hyperplane. Once the trajectory is on the discontinuity hyperplane, smooth closed-loop system dynamics can be restored and standard Lyapunov theory can be used.

The linear boundedness of controller (22) prevents the state of the closed-loop system (20)–(22), from escaping to infinity in finite time. Subject to the lower bound (23), this controller dominates the rest, $(A_{21} - KA_{11})\xi_1 + (A_{22} - KA_{12})\xi_2$, of the right-hand side of the equation

$$\sigma\dot{\xi} = (A_{21} - KA_{11})\xi_1 + (A_{22} - KA_{12})\xi_2 + B_{12}u(\xi) \tag{26}$$

thereby providing the flow of the closed-loop system to be directed toward the discontinuity hyperplane $\sigma\xi = 0$. Since the sliding mode equation $\sigma\dot{\xi} = 0$, or equivalently

$$\dot{\xi}_1 = (A_{11} + A_{12}K)\xi_1 \tag{27}$$

is exponentially stable due to a special choice of K, the finite-dimensional system (20) and (21), driven by the discontinuous control law (22)–(25), can be proven to be asymptotically (when $\gamma_0 > 0$) or exponentially stable (when $\gamma_0 = 0$).

The following result is inspired from the standard sliding-mode control theory (Utkin 1992, Chapter 7, § 6)

Lemma 1: *Let the finite-dimensional system* (20) *and* (21), *be driven by the unit control law* (22)–(25). *Then, given an initial condition* $\xi(0) = \xi^0 \in R^n$, *the closed-loop system* (20)–(25) *has a unique solution, globally defined for all* $t \ge 0$, *and this system is globally asymptotically stable when* $\gamma_0 > 0$ *and it is globally exponentially stable when* $\gamma_0 = 0$.

Proof: We break up the proof into three simple steps.

(1) By the theorem of Utkin (1992, p. 16) a unique solution of the finite-dimensional system (20)–(25) exists locally for all initial conditions. By the same theorem, a system motion on the discontinuity hyperplane $\sigma\xi = 0$, if any, is governed by the sliding mode equation (27). While being governed by the linear equation (27), such a motion is apparently uniformly bounded on an arbitrary finite time interval and globally continuable on the right. The same is also true for a motion, initialized beyond the discontinuity hyperplane.

Indeed, beyond this hyperplane the right-hand side of the state equation (20)–(25) is linearly bounded in the state variable so that

$$\|\xi(t)\| \leq \|\xi^0\| + \int_0^t [\gamma_0 + L\|\xi(\tau)\|] \, d\tau \tag{28}$$

for some constant $L > 0$. It follows that

$$\|\xi(t)\| \leq [\|\xi^0\| + \gamma_0 T] + L \int_0^t \|\xi(\tau)\| \, d\tau, \ 0 \leq t < T. \tag{29}$$

By applying the Bellman–Gronwall lemma to inequality (29), any solution of this equation is uniformly bounded

$$\|\xi(t)\| \leq [\|\xi^0\| + \gamma_0 T] \, e^{LT} \tag{30}$$

on an arbitrary time interval $[0, T)$ before possible getting on the discontinuity hyperplane where it has been shown to remain uniformly bounded on any finite time interval. Thus, given an arbitrary initial condition, there exists a unique solution of (20)–(25), which turns out to be globally continuable on the right.

(2) Let us now assume that $\gamma_0 > 0$ and let us demonstrate that the closed-loop system in this case is globally asymptotically stable. For this purpose, we introduce the quadratic function

$$V(\sigma\xi) = (\sigma\xi)^{\mathrm{T}} \sigma\xi \tag{31}$$

and compute its time derivative along the trajectories of the closed-loop system (20)–(25)

$$\begin{aligned} \dot{V}(t) = {} & 2(\sigma\xi)^{\mathrm{T}}\{(A_{21} - KA_{11})\xi_1 + (A_{22} - KA_{12})\xi_2 \\ & - [\gamma_0 + \gamma_1\|\xi\|]U(\sigma\xi)\} \leq -2(\sigma\xi)^{\mathrm{T}}\{\gamma_0 + [\gamma_1 - \|A_{21} \\ & - KA_{11}\| - \|A_{22} - KA_{12}\|]\|\xi\|\} \frac{\sigma\xi}{\|\sigma\xi\|}. \end{aligned} \tag{32}$$

Due to (23), it follows that

$$\dot{V}(t) \leq -2\gamma_0\|\sigma\xi\| = -2\gamma_0\sqrt{V(t)} \tag{33}$$

thereby yielding the finite time convergence of $V(t)$ to zero. In order to reproduce this conclusion, one should note that for all $t \geq 0$, an arbitrary solution $V(t)$ to the latter inequality is dominated, i.e. $V(t) \leq V_0(t)$, by the solution to the differential equation $\dot{V}_0(t) = -2\gamma_0\sqrt{V_0(t)}$, initialized with the same initial condition $V_0(0) = \|\sigma\xi^0\|^2$. Since $V_0(t) = 0$ for all $t \geq \gamma_0^{-1} \| \times \sigma\xi^0\|$, $V(t)$ vanishes after a finite time moment $T \leq T_0 = \gamma_0^{-1}\|\sigma\xi^0\|$, i.e. $\sigma\xi(t) = 0$ for all $t \geq T$.

Thus, starting from the finite time moment $T \leq \gamma_0^{-1}\|\sigma\xi^0\|$ the closed-loop system evolves in the sliding mode on the m-dimensional hyperplane $\sigma\xi = 0$. By the theorem of Utkin (1992, p. 16), this motion is governed by the sliding mode equation (27) which is globally exponentially stable due to a special choice of the matrix K. While being governed on the time interval $t \in [0, T)$ by the ordinary differential equations (20) and (21) with a smooth right-hand side, the initial stage of the trajectory, before it hits the discontinuity hyperplane $\sigma\xi = 0$, continuously depends on the initial conditions. Coupled to the exponential stability of the sliding motion after the time moment T, this ensures the closed-loop system (20)–(25) with $\gamma_0 > 0$ to be globally asymptotically stable on the semi-infinite time interval $[0, \infty)$.

(3) Setting $\gamma_0 = 0$ in the control algorithm (22), the derivative estimate (32) for the quadratic function (31) takes the form

$$\dot{V}(t) \leq -2\gamma\|\xi(t)\|\sqrt{V(t)} \tag{34}$$

where $\gamma = \gamma_1 - \|A_{21} - KA_{11}\| - \|A_{22} - KA_{12}\|$ is positive by virtue of (23).

In contrast to (33), equality (34) cannot guarantee that $V(t) = 0$ starting from a finite time moment because (23) is now violated for $\|\xi(t)\| \to 0$. However, if for some $\zeta \in (0, 1)$ the state estimate

$$\|\xi(t)\| > \zeta\|\xi^0\| \tag{35}$$

could be guaranteed on the time interval $t \in (0, T)$ with

$$T = \frac{\|\sigma\xi^0\|}{\gamma\zeta\|\xi^0\|} \tag{36}$$

then in analogy to (33), the trajectory of the closed-loop system (20)–(25), corresponding to $\gamma_0 = 0$, would also enter the hyperplane $\sigma\xi = 0$ in a finite time $\tau_0 \leq T$, and starting from τ_0 the system would evolve in the sliding mode on this hyperplane.

If hypothesis (35) fails to hold on the entire time interval $(0, \tau_0)$, then there exists a time moment $t_1 \in (0, \tau_0)$ such that

$$\|\xi(t_1)\| = \zeta\|\xi^0\|. \tag{37}$$

Taking into account the earlier obtained state estimate (30) subject to $\gamma_0 = 0$, it follows that

$$\|\xi(t)\| \leq \|\xi^0\| \, e^{LT} \quad \text{for} \quad t \in (0, t_1). \tag{38}$$

Now regarding t_1 as the new initial time moment and following the same line of reasoning as before, we can obtain that either the state vector enters the hyperplane $\sigma\xi = 0$ at time instant $\tau_1 < t_1 + T$ and then it evolves in the sliding mode on this hyperplane, or $\|\xi(t_2)\| = \zeta^2\|\xi^0\|$ for some $t_2 \in (t_1, \tau_1)$ and

$$\|\xi(t)\| \leq \zeta\|\xi^0\| \, e^{LT} \quad \text{for } t \in (t_1, t_2). \tag{39}$$

Thus, by iterating on i, we conclude that either the state vector enters the hyperplane $\sigma\xi = 0$ in a finite time and after that it never leaves this hyperplane, or $\|\xi(t_{i+1})\| = \zeta^{i+1}\|\xi^0\|$ for some $t_{i+1} \in (t_i, \tau_i)$, $i = 0, 1, \ldots,$ and

$$\|\xi(t)\| \leq \zeta^i\|\xi^0\| \, e^{LT} \quad \text{for} \quad t \in (t_i, t_{i+1}) \tag{40}$$

where $t_0 = 0$.

In the latter case, inequalities (2), coupled together for $i = 0, 1, \ldots,$ ensure that for all $t \geq 0$ there exists a decaying exponential state estimate

$$\|\xi(t)\| \leq L_0\|\xi^0\| e^{-\mu t} \tag{41}$$

with $\mu = -T^{-1}\ln\zeta > 0$ and $L_0 = e^{LT} > 0$.

In turn, in the former case, inequalities (41) are also satisfied before the instant of hitting the hyperplane $\sigma\xi = 0$ whereas after this instant the sliding motion on $\sigma\xi = 0$ is governed by the globally exponentially stable equation (27). Thus, in any case the closed-loop system (20)–(25) with $\gamma_0 = 0$ proves to be globally exponentially stable. Lemma 1 is completely proven.

One can be surprised that according to Lemma 1, feedback (22) with $\gamma_0 > 0$ can only guarantee asymptotic stability of the closed-loop system whereas the less powerful feedback (22) with $\gamma_0 = 0$ exponentially stabilizes the system. To explain this, one should take into account that the peaking phenomenon (Sussman and Kokotovic 1991) in the initial stage of the trajectory, before it hits the discontinuity hyperplane, is capable of destroying exponential stability of the system, but it can only occur when $\gamma_0 > 0$ (cf. the general upper estimate (30) and the particular upper estimate (41), corresponding to $\gamma_0 = 0$).

Remark 2: It is worth noting that the sign of the time derivative (32) of the quadratic function (31), computed along the trajectories of the closed-loop system (20)–(25) with $\gamma_0 > 0$, remains negative even in the case when sufficiently small matched disturbances $d(x, t) \in R^m$, which satisfy $\|d(\xi, t)\| < \gamma_0$ for all $\xi \in R^n$ and all $t > 0$, affect the system. Thus, the line of reasoning, used in the proof of Lemma 1, applies to such a perturbed system as well, so that the matched disturbances are rejected by the unit controller (22)–(25) with γ_0 exceeding a norm bound of these disturbances (see also the example § 4.2).

Remark 3: The main drawback of the use of the unit controller (22)–(25) with positive γ_0 is that of fast switching of the control action in a practical implementation of such a controller; this may excite unmodelled high-frequency dynamics of the closed-loop system that may severely limit the achievable closed-loop performance. A continuous version of this controller can be obtained for $\gamma_0 = 0$ (note that in the particular case, where the number of the control inputs, m, equals to the dimension of the system, n, the resulting controller will also be linear). While being continuous in the origin, this controller reduces the amplitude of undesired oscillations around the equilibrium solution, however, in contrast to its counterpart with positive γ_0, it cannot reject non-vanishing disturbances.

In what follows, we demonstrate that the same control law (22)–(25) globally stabilizes (asymptotically (when $\gamma_0 > 0$) or exponentially (when $\gamma_0 = 0$)) the closed-loop infinite-dimensional system (1).

Theorem 2: *Consider an infinite-dimensional system* (1) *for which Assumption* 1 *holds and let the unit control signal* (22)–(25) *be constructed via the finite-dimensional approximation* (10) *of the system and its equivalent representation* (18)–(21). *Then, given an initial condition* $x(0) = x^0 \in H$, *the closed-loop system* (1) *and* (22)–(25) *has a unique solution, which is globally defined for all* $t \geq 0$, *and this system is globally asymptotically stable when* $\gamma_0 > 0$ *and it is globally exponentially stable when* $\gamma_0 = 0$.

Proof: The proof follows the same path as in Lemma 1.

(1) By Lemma 1, a unique solution of the finite-dimensional system (20)–(25) exists for all initial conditions and this solution is globally defined for all $t \geq 0$. While this system remains beyond the discontinuity hyperplane $\sigma\xi = 0$, the control function $u(t)$, computed according to (22) on the trajectories of (20) and (21), is continuously differentiable in t. Thus, before the solution of the finite-dimensional system (20)–(25) hits the discontinuity hyperplane, the infinite-dimensional system (11), driven by this control signal, satisfies Pazy (1983, p. 109, Corollary 2.10). By this corollary, system (11) and (22) has a unique solution under arbitrary initial conditions (3) at least till a time instant when system (20)–(25) enters the hyperplane $\sigma\xi = 0$.

As shown in the proof of Lemma 1, any solution of the finite-dimensional system (20)–(25), entering the discontinuity hyperplane in a finite time $T > 0$, never leaves it. In order to describe the behaviour of the infinite-dimensional system (11) and (22) on the hyperplane $\sigma\xi = 0$, one should use the infinite-dimensional extension of the equivalent control method that has recently been justified in Orlov (2000). According to this extension, the equivalent control value

$$u_{eq} = B_{12}^{-1}(KA_{11} + KA_{12}K - A_{21} - A_{22}K)\xi_1 \quad (42)$$

a unique solution of the equation $\dot{\sigma}(\xi(t)) = 0$ with respect to u, is substituted into (11) for u. By Orlov (2000, theorem 1), the equation

$$\dot{x}_2 = A_2x_2 + B_2B_{12}^{-1}(KA_{11} + KA_{12}K - A_{21} - A_{22}K)\xi_1, \ t \geq T, \quad (43)$$

thus obtained, describes the motion of the infinite-dimensional subsystem (11) while the finite-dimensional subsystem (10) evolves in the sliding mode on the discontinuity hyperplane $\sigma\xi = 0$.

Apparently, the equivalent control function (42), computed along the sliding modes (27), is continuously differentiable in t, and hence, the infinite-dimensional sliding mode equation (43) satisfies Pazy (983, p.109, Corollary 2.10), too. By applying this corollary to (43), we conclude that the solutions of the infinite-dimensional part (11) and (22) of the closed-loop system (1) and (22)–(25) are globally continuable on the right, even if the finite-dimensional system enters the discontinuity hyperplane $\sigma\xi = 0$ in a finite time.

(2) If $\gamma_0 > 0$ then, as shown in the proof of Lemma 1, after the finite time $T \leq \gamma_0^{-1}\|\sigma\xi^0\|$ the finite-dimensional system (20)–(25) evolves in the sliding mode on the hyperplane $\sigma\xi = 0$. While being governed on the time interval $[0, T)$ by the differential equations (11), (20) and (25), subject to the smooth control input (22), the initial stage of the trajectory $x(t)$, before it hits the discontinuity hyperplane $\sigma\xi = 0$, continuously depends on the initial data x^0.

In turn, for $t \geq T$ the closed-loop system (1), (22)–(25) is maintained on the hyperplane $\sigma\xi = 0$ and it is governed by the sliding mode equations (27) and (43). Due to a special choice of K, the solution of the former equation is exponentially decaying

$$\|\xi_1(t)\| \leq \omega\|\xi_1(T)\|e^{-\beta(t-T)}, \quad t \geq T \quad (44)$$

with some $\omega > 0$ and $\beta > 0$. Since the semigroup $S_{A_2}(t)$ generated by the infinitesimal operator A_2 is exponentially stable, i.e. $\|S_{A_2}(t-T)\| \leq \omega_0 e^{-\alpha(t-T)}$ for all $t \geq T$ and some $\alpha, \omega_0 > 0$, the solution of the latter equation, given by

$$x_2(t) = S_{A_2}(t-T)x_2(T) + \int_T^t S_{A_2}(t-T-\tau)B_2B_{12}^{-1} \times (KA_{11} + KA_{12}K - A_{21} - A_{22}K)\xi_1(\tau)\,d\tau \quad (45)$$

is estimated as

$$\|x_2(t)\| \leq \omega_0\|x_2(T)\|e^{-\alpha(t-T)} + \kappa\|\xi_1(T)\|[e^{-\beta(t-T)} + e^{-\alpha(t-T)}], \ t \geq T \quad (46)$$

where

$$\kappa = \frac{\omega_0\omega e^{\alpha T}}{|\alpha - \beta|} \times \|B_2B_{12}^{-1}(KA_{11} + KA_{12}K - A_{21} - A_{22}K)\| > 0$$

and inequality (44) has been used. By taking into account (44) and employing that $\sigma\xi = 0$, or equivalently, $\xi_2(t) = K\xi_1(t)$ for $t \geq T$, it follows that

$$\|x(t)\| \leq \omega_1\|x(T)\|e^{-\nu_1(t-T)}, \quad t \geq T \quad (47)$$

for some $\omega_1 > 0$ and $\nu_1 > 0$. Coupled to the afore-mentioned property of the initial stage of the solution to continuously depend on the initial data, the exponential decay (47) after the finite time moment T ensures the global asymptotic stability of the closed-loop system (1), (22)–(25) with $\gamma_0 > 0$.

(3) If $\gamma_0 = 0$ then apart from the exponential decay (3) on the discontinuity hyperplane $\sigma\xi = 0$, a similar state estimate takes place at the initial stage preceding a sliding motion on this hyperplane. Indeed, by Lemma 1, the finite-dimensional component ξ(t) of the closed-loop system (1) and (22)–(25) with $\gamma_0 = 0$ is globally exponentially stable whereas the solution

$$x_2(t) = S_{A_2}(t)x_2(0) - \gamma_1\int_0^t \|\xi(\tau)\|S_{A_2}(t-\tau)B_2B_{12}^{-1} \times \frac{\sigma\xi(\tau)}{\|\sigma\xi(\tau)\|}\,d\tau, \ 0 \leq t < T \quad (48)$$

of the infinite-dimensional part (11), before $\xi(t)$ hits the hyperplane $\sigma\xi = 0$, is estimated as

$$\|x_2(t)\| \leq \omega_0\|x_2(0)\|e^{-\alpha t} + \kappa_1\|\xi^0\|[e^{-\mu t} + e^{-\alpha t}], \quad 0 \leq t < T \quad (49)$$

where

$$\kappa_1 = \frac{L_0\omega_0\gamma_1}{|\alpha - \mu|}\|B_2B_{12}^{-1}\| > 0$$

and inequality (41) has been used. By taking into account (41), it follows that

$$\|x(t)\| \leq \omega_2\|x^0\|e^{-\nu_2 t}, \quad 0 \leq t < T \quad (50)$$

for some $\omega_2 > 0$ and $\nu_2 > 0$. Since relation (50), coupled to (47), ensures that

$$\|x(t)\| \leq \Omega\|x^0\|e^{-\nu t}, \ t \geq 0 \quad (51)$$

for $\Omega = \max\{\omega_1, \omega_2, \omega_1\omega_2\} > 0$ and $\nu = \min\{\nu_1, \nu_2\} > 0$, regardless of whether the closed-loop system enters the discontinuity hyperplane $\sigma\xi = 0$ in a finite time $T < \infty$ or it never hits this hyperplane, the global exponential stability of (1) and (22)–(25) with $\gamma_0 = 0$ is guaranteed. Thus, Theorem 2 is completely proven. □

The implementation of the discontinuous unit feedback (25) can be performed through its continuous approximation $U^\delta(\sigma\xi)$, e.g.

$$U^\delta(\sigma\xi) = \frac{\sigma\xi}{\|\sigma\xi\| + \delta^3} \tag{52}$$

such that condition (5) holds with $u(x) = \sigma\xi/\|\sigma\xi\|$ and $u^\delta(x) = U^\delta(\sigma\xi)$. Undesirable high frequency state oscillations that would be excited by fast switching in the discontinuous controller are thus avoided, and the resulting closed-loop system, corresponding to a sufficiently small δ, can be shown to be practically stable (i.e. all the trajectories converge to an ϵ-vicinity of the equilibrium solution). Theorem 3 summarizes the main result.

Theorem 3: *Let a continuous approximation* (52) *of the discontinuous unit feedback signal* (25) *be substituted into the control law* (22) *for* $U(\sigma x)$. *Then, given an initial condition* (3) *and sufficiently small* $\delta > 0$, *the closed-loop system* (1) *and* (22)–(24) *and* (52) *has a unique solution* $x^\delta(t)$, *globally defined for all* $t \geq 0$. *Moreover, this system is Lyapunov stable, and for arbitrary* $\epsilon > 0$ *there exist* $\delta_0(\epsilon)$ *and* $T_0(x^0, \epsilon) > 0$ *such that*

$$\|x^\delta(t)\| < \epsilon \quad \text{for all} \quad t \geq T_0(x^0, \epsilon) \text{ and } \delta \in (0, \delta_0) \tag{53}$$

Proof: By Theorem 2 system (1) and (3), driven by the discontinuous controller (22)–(25), has a unique solution $x(t)$, globally defined for all $t \geq 0$, and $x(t) \to 0$ as $t \to \infty$. The latter guarantees that for arbitrary $\epsilon > 0$ there exists $T_0(x^0, \epsilon) > 0$ such that

$$\|x(t)\| \leq \frac{\epsilon}{2} \quad \text{for all} \quad t \geq T_0(x^0, \epsilon). \tag{54}$$

In turn, the smoothed system (1) and (3), driven by the continuous, piece-wise smooth controller (22)–(24) and (52), is well-known (Pazy 1983) to have a unique solution $x^\delta(t)$, locally defined on some time interval $(0, \tau)$. Then Theorem 1 and Definition 2, coupled together, ensure that

$$\|x(t) - x^\delta(t)\| \leq \frac{\epsilon}{2} \quad \text{for all} \quad t \in (0, \tau), \ \delta \in (0, \delta_0) \tag{55}$$

and some $\delta_0(\epsilon) > 0$. Thus, the solutions $x^\delta(t)$ are uniformly bounded on $(0, \tau)$ for all $\delta \in (0, \delta_0)$, and these solutions are therefore uniquely continuable on the right so that inequality (55) remains in force for $t \geq \tau$. By virtue of (54), it follows stability of the closed-loop system (1), (22)–(24), (52) and validity of (53). Theorem 3 is proven. □

We note that Remarks 2 and 3 apply to the infinite-dimensional system (1) as well. In § 4, these conclusions will be supported by numerical simulations.

3.2. *Output feedback design*

In this subsection, we proceed with the design of the discontinuous output feedback controller by coupling the discontinuous state feedback law (22) with the Luenberger observer (14) and (15). For this purpose, we first represent (22) in terms of the state component x_1

$$u(x_1) = -[\gamma_0 + \gamma_1\|Mx_1\|]B_{12}^{-1}\frac{(P_{12} - KP_{11})Mx_1}{\|(P_{12} - KP_{11})Mx_1\|}. \tag{56}$$

Then, we substitute x_1 by the observer output $\tilde{x}_1$ in (56) and modify the gain $\gamma_0 + \gamma_1\|M\tilde{x}_1\|$ by adding the error term $\gamma_2\|y - C\tilde{x}\|$ with

$$\gamma_2 > \|(P_{12} - KP_{11})L_1\|. \tag{57}$$

The reason for the gain modification is to ensure that the observer-based controller is capable of steering the trajectories of the closed-loop system to the discontinuity manifold $(P_{12} - KP_{11})M\tilde{x}_1 = 0$ in spite of the observer error, thereby imposing on the system a desired stability property similar to that obtained under the state feedback controller. By Theorem 4, stated below, the resulting discontinuous output feedback control law, which yields a proper solution to the stabilization problem in question, takes the form

$$u(y, \tilde{x}) = -[\gamma_0 + \gamma_1\|M\tilde{x}_1\| + \gamma_2\|y - C\tilde{x}\|]B_{12}^{-1}\frac{(P_{12} - KP_{11})M\tilde{x}_1}{\|(P_{12} - KP_{11})M\tilde{x}_1\|}. \tag{58}$$

Theorem 4: *Let the infinite-dimensional system* (1) *for which Assumption* 1 *holds be driven by the observer-based dynamic output feedback controller* (14), (15) *and* (58) *with gain parameters* γ_0, γ_1 *and* γ_2, *satisfying* (23) *and* (57), *respectively. Then, given initial conditions* $x(0) = x^0 \in H$, $\tilde{x}(0) = \tilde{x}^0 \in H$, *the closed-loop system* (1), (14), (15) *and* (58) *has a unique solution, globally defined for all* $t \geq 0$, *and this system is globally asymptotically stable when* $\gamma_0 > 0$ *and it is globally exponentially stable when* $\gamma_0 = 0$.

Proof: The proof parallels that of Theorem 2.

(1) First let us represent the over-all system (1), (14), (15) and (58) in terms of the observer error $e = (e_1, e_2)^{\mathrm{T}}$, $e_i = x_i - \tilde{x}_i$, $i = 1, 2$, and

the observer state components $\tilde{\xi} = (\tilde{\xi}_1, \tilde{\xi}_2)^T$, $\tilde{\xi}_i = P_{1i} M \tilde{x}_1$ and $\tilde{x}_2$

$$\dot{e}_1 = (A_1 + L_1 C_1) e_1 + L_1 C_2 e_2$$
$$\dot{e}_2 = A_2 e_2 \tag{59}$$

$$\dot{\tilde{\xi}}_1 = A_{11}\tilde{\xi}_1 + A_{12}\tilde{\xi}_2 - P_{11} L_1 C e \tag{60}$$

$$\dot{\tilde{\xi}}_2 = A_{21}\tilde{\xi}_1 + A_{22}\tilde{\xi}_2 + B_{12} u(y, \tilde{\xi}, \tilde{x}_2) - P_{12} L_1 C e \tag{61}$$

$$\dot{\tilde{x}}_2 = A_2 \tilde{x}_2 + B_2 u(y, \tilde{\xi}, \tilde{x}_2) \tag{62}$$

where

$$u(y, \tilde{\xi}, \tilde{x}_2) = -\Big[\gamma_0 + \gamma_1 \|\tilde{\xi}\| + \gamma_2 \|y - C_1 M^{-1}\tilde{\xi} - C_2 \tilde{x}_2\|\Big] B_{12}^{-1} \frac{\sigma\tilde{\xi}}{\|\sigma\tilde{\xi}\|} \tag{63}$$

and $\sigma\tilde{\xi} = \tilde{\xi}_2 - K\tilde{\xi}_1$.

Since the semigroup $S_{A_2}(t)$ generated by the infinitesimal operator A_2 is exponentially stable and $A_1 + L_1 C_1$ is a Hurwitz matrix by construction, the observer error equation (59) has a unique globally defined solution under arbitrary initial conditions $e_1(0) = e_1^0 \in R^n$, $e_2(0) = e_2^0 \in H$ and this solution is given by

$$e_1(t) = \mathrm{e}^{(A_1 + L_1 C_1)t} \mathrm{e}_1^0 + \int_0^t \mathrm{e}^{(A_1 + L_1 C_1)(t-\tau)} \times L_1 C_2 S_{A_2}(\tau)\, \mathrm{e}_2^0 \, \mathrm{d}\tau \tag{64}$$

$$e_2(t) = S_{A_2}(t)\, \mathrm{e}_2^0, \quad t \geq 0. \tag{65}$$

The following observer error estimate

$$\|e(t)\| \leq \kappa_0 \|e(0)\| \mathrm{e}^{-\beta_0 t}, \quad t \geq 0, \quad i = 1, 2 \tag{66}$$

is then straightforwardly obtained for some positive κ_0 and β_0.

It follows that subsystem (60)–(63) is enforced by the exponentially decaying inputs $P_{11} L_1 Ce(t)$ and $P_{12} L_1 Ce(t)$. While subsystem (60)–(63) remains beyond the discontinuity hyperplane $\sigma\tilde{\xi} = 0$, the control function $u(t)$, computed according to (63) on the trajectories of (60)–(62), is continuously differentiable in t. Thus, before the subsystem hits the discontinuity hyperplane, it satisfies Pazy (1983, p. 109, Corolarry 2.10). By this corollary, subsystem (60)–(63) has a unique solution under arbitrary initial conditions at least till a time instant when the subsystem enters the hyperplane $\sigma\tilde{\xi} = 0$.

It should be noted that if subsystem (60)–(63) enters the discontinuity hyperplane then it never leaves it because the time derivative of the quadratic function

$$V(\sigma\tilde{\xi}) = (\sigma\tilde{\xi})^T \sigma\tilde{\xi} \tag{67}$$

remains negative on the trajectories of the system beyond this hyperplane

$$\dot{V}(t) = \leq -2(\sigma\tilde{\xi})^T (\gamma_0 + \gamma\|\tilde{\xi}\| + \tilde{\gamma}\|e\|) \frac{\sigma\tilde{\xi}}{\|\sigma\tilde{\xi}\|} \tag{68}$$

where constants $\gamma = \gamma_1 - \|A_{21} - KA_{11}\| - \|A_{22} - KA_{12}\|$ and $\tilde{\gamma} = (\gamma_2 - \|(P_{12} - KP_{11})L_1\|)\| \, C\|$ are positive by virtue of (23) and (57).

In order to describe the behaviour of subsystem (60)–(63) on the hyperplane $\sigma\tilde{\xi} = 0$, one should use the infinite-dimensional extension of the equivalent control method (Orlov 2000). According to this extension, the equivalent control value

$$u_{eq} = B_{12}^{-1}[(KA_{11} + KA_{12}K - A_{21} - A_{22}K)\tilde{\xi}_1 + (P_{12} - KP_{11}) L_1 Ce] \tag{69}$$

a unique solution of the equation $\dot{\sigma}(\tilde{\xi}(t)) = 0$ with respect to u, is substituted into (61) and (62) for u. By Orlov (2000, theorem 1), the equations

$$\dot{\tilde{\xi}}_1 = (A_{11} + KA_{12})\tilde{\xi}_1 - P_{11} L_1 Ce \tag{70}$$

$$\dot{\tilde{x}}_2 = A_2 \tilde{x}_2 + B_2 B_{12}^{-1}(KA_{11} + KA_{12}K - A_{21} - A_{22}K)\tilde{\xi}_1 + B_2 B_{12}^{-1}(P_{12} - KP_{11}) L_1 Ce \tag{71}$$

thus obtained, describe the motion of subsystem (60)–(63) after a time instant when the subsystem hits the discontinuity hyperplane $\sigma\tilde{\xi} = 0$.

While being governed by the linear equation (70) subject to (66), the finite-dimensional component $\tilde{\xi}(t)$ of the sliding motion is apparently uniformly bounded on an arbitrary finite time interval and globally continuable on the right. The same is also true for a motion, initialized beyond the discontinuity hyperplane. Indeed, beyond this hyperplane the right-hand side of (60), (61) and (63) is linearly bounded in the state variable so that

$$\|\tilde{\xi}(t)\| \leq \|\tilde{\xi}^0\| + \int_0^t [\gamma_0 + N_1 \|\tilde{\xi}(\tau)\| + N_2 \|e(\tau)\|] \, \mathrm{d}\tau \tag{72}$$

for some constants $N_1, N_2 > 0$. Taking into account (66), it follows that

$$\|\tilde{\xi}(t)\| \leq [\|\tilde{\xi}^0\| + \frac{\kappa_0 N_2}{\beta_0} \|e^0\| + \gamma_0 T] + N_1 \int_0^t \|\tilde{\xi}(\tau)\| \mathrm{d}\tau \tag{73}$$

By applying the Bellman–Gronwall lemma to inequality (73), any solution of this equation is uniformly bounded

$$\|\tilde{\xi}(t)\| \le [\|\tilde{\xi}^0\| + \frac{\kappa_0 N_2}{\beta_0}\|e^0\| + \gamma_0 T]\,\mathrm{e}^{N_1 T} \qquad (74)$$

on an arbitrary time interval $[0, T)$ before possible getting on the discontinuity hyperplane where it has been shown to remain uniformly bounded on any finite time interval. Thus, given arbitrary initial conditions $e^0 \in H$, $\tilde{\xi}^0 \in R^n$, there exists a unique solution of (59)–(61) and (63), which turns out to be globally continuable on the right.

Moreover, the equivalent control function (69), computed along the sliding modes (70), is continuously differentiable in t, and hence, the infinite-dimensional sliding mode equation (71) satisfies Pazy (1983, p. 109, Corollary 2.10). By applying this corollary to (71), we conclude that the solutions of the infinite-dimensional part (62) and (63) of the closed-loop system (59)–(63) are unambiguously globally continuable on the right, even if the finite-dimensional system enters the discontinuity hyperplane $\sigma\tilde{\xi} = 0$ in a finite time.

Since (59)–(63) is nothing else than a representation of the original closed-loop system (1), (14), (15) and (58) in terms of the observer error and observer state, a solution of the original system is globally uniquely defined, too.

(2) If $\gamma_0 > 0$ then the time derivative estimate (33) of the quadratic function (67) is now guaranteed by (68). As shown in the proof of Lemma 1, this estimate ensures that $V(t) = 0$ for all $t \ge \gamma_0^{-1}\ \|\sigma\tilde{\xi}^0\|$, i.e. after a finite time moment $T \le \gamma_0^{-1}\ \|\sigma\tilde{\xi}^0\|$ the finite-dimensional system (60), (61) and (63) evolves in the sliding mode on the hyperplane $\sigma\tilde{\xi} = 0$. While being governed on the time interval $t \in [0, T)$ by the differential equations (59)–(62) subject to the smooth control input (63), the initial stage of the trajectory of the system, before it hits the discontinuity hyperplane $\sigma\tilde{\xi} = 0$, continuously depends on the initial conditions.

In turn, for $t \ge T$ the closed-loop system (59)–(63) is maintained on the hyperplane $\sigma\tilde{\xi} = 0$ and it is governed by the sliding mode equations (70) and (71). Taking into account the observer error estimate (66) and employing that $A_{11} + KA_{12}$ is a Hurwitz matrix due to a special choice of K, the solution of the former equation is proven to exponentially decay with some $\omega > 0$ and $\beta > 0$

$$\|\tilde{\xi}_1(t)\| \le \omega\|\tilde{\xi}_1(T)\|\mathrm{e}^{-\beta(t-T)}, \quad t \ge T. \qquad (75)$$

Since the semigroup $S_{A_2}(t)$ generated by the infinitesimal operator A_2 is exponentially stable, i.e. $\|S_{A_2}(t-T)\| \le \omega_0\,\mathrm{e}^{-\alpha(t-T)}$ for all $t \ge T$ and some $\alpha, \omega_0 > 0$, the solution of the latter equation, given by

$$\begin{aligned}\tilde{x}_2(t) = {} & S_{A_2}(t-T)\tilde{x}_2(T) \\ & + \int_T^t S_{A_2}(t-T-\tau)B_2B_{12}^{-1}(P_{12} - KP_{11}) \\ & \times L_1Ce(\tau)\,\mathrm{d}\tau + \int_T^t S_{A_2}(t-T-\tau)B_2B_{12}^{-1} \\ & \times (KA_{11} + KA_{12}K - A_{21} - A_{22}K)\xi_1(\tau)\,\mathrm{d}\tau \end{aligned} \qquad (76)$$

is estimated as

$$\begin{aligned}\|\tilde{x}_2(t)\| \le {} & \omega_0\|\tilde{x}_2(T)\|\,\mathrm{e}^{-\alpha(t-T)} \\ & + \tilde{\kappa}\|e(T)\|\Big[\mathrm{e}^{-\beta_0(t-T)} + \mathrm{e}^{-\alpha(t-T)}\Big] \\ & + \kappa\|\xi_1(T)\|\Big[\mathrm{e}^{-\beta(t-T)} + \mathrm{e}^{-\alpha(t-T)}\Big], \quad t \ge T \end{aligned} \qquad (77)$$

where

$$\tilde{\kappa} = \frac{\omega_0\kappa_0\mathrm{e}^{\alpha T}}{|\alpha - \beta_0|}\|B_2B_{12}^{-1}(P_{12} - KP_{11})L_1C\| > 0$$

$$\kappa = \frac{\omega_0\omega\mathrm{e}^{\alpha T}}{|\alpha - \beta|}\|B_2B_{12}^{-1}(KA_{11} + KA_{12}K - A_{21} - A_{22}K)\| > 0,$$

and inequalities (66) and (75) have been used. By taking into account (66)–(75), and employing that $\sigma\tilde{\xi} = 0$, or equivalently, $\tilde{\xi}_2(t) = K\tilde{\xi}_1(t)$ for $t \ge T$, it follows that in the case when $\gamma_0 > 0$ the closed-loop system (59)–(63) is exponentially decaying for $t \ge T$. Coupled to the afore-mentioned property of the initial stage of the solution to continuously depend on the initial conditions, this ensures the global asymptotic stability of (59)–(63) as well as that of the original closed-loop system (1), (14), (15) and (58) whenever $\gamma_0 > 0$.

(3) For later use, we present the following extension of Lemma 1. □

Lemma 2: *Let the finite-dimensional system* (60) *and* (61) *be enforced by the unit controller* (63) *subject to* $\gamma_0 = 0$ *and let the exponential estimate* (66) *hold for the input signal. Then, the closed-loop system is globally exponentially stable.*

Proof: The proof is nearly the same as that of Lemma 1 and it is therefore omitted. □

If $\gamma_0 = 0$ then apart from the exponential decaying of the closed-loop system (59)–(63) on the discontinuity hyperplane $\sigma\tilde{\xi} = 0$, this is also true at the initial stage preceding a sliding motion on this hyperplane. Indeed, by Lemma 2, the finite-dimensional component $\tilde{\xi}(t)$ of (59)–(63) with $\gamma_0 = 0$ is globally exponentially stable

$$\|\tilde{\xi}(t)\| \leq L_0 \|\tilde{\xi}(0)\| e^{-\mu t}, \quad t \geq 0 \tag{78}$$

for some $\mu > 0$ and $L_0 > 0$, whereas the solution

$$\tilde{x}_2(t) = S_{A_2}(t)\tilde{x}_2(0) - \int_0^t [\gamma_1 \|\tilde{\xi}(\tau)\| + \gamma_2 \|Ce(\tau)\|] S_{A_2}(t-\tau) \times B_2 B_{12}^{-1} \frac{\sigma\tilde{\xi}(\tau)}{\|\sigma\tilde{\xi}(\tau)\|} \, \mathrm{d}\tau, \; 0 \leq t < T \tag{79}$$

of the infinite-dimensional part (15), before the time instant T when $\tilde{\xi}(t)$ hits the hyperplane $\sigma\tilde{\xi} = 0$, is estimated as

$$\|\tilde{x}_2(t)\| \leq \omega_0 \|\tilde{x}_2(0)\| \mathrm{e}^{-\alpha t} + \kappa_1 \|\tilde{\xi}(0)\| [\mathrm{e}^{-\mu t} + \mathrm{e}^{-\alpha t}] + \kappa_2 \|e(0)\| [\mathrm{e}^{-\beta_0 t} + \mathrm{e}^{-\alpha t}], \quad 0 \leq t < T \tag{80}$$

where

$$\kappa_1 = \frac{L_0 \omega_0 \gamma_1}{|\alpha - \mu|} \|B_2 B_{12}^{-1}\| > 0,$$
$$\kappa_2 = \frac{\kappa_0 \omega_0 \gamma_2}{|\alpha - \beta_0|} \|B_2 B_{12}^{-1}\| \|C\| > 0$$

and inequalities (66) and (78) have been used. As in the proof of Theorem 1, relations (77) and (80), coupled together, ensure that the infinite-dimensional part (15) is also exponentially stable, regardless of the closed-loop system (59)–(63) enters the discontinuity hyperplane $\sigma\tilde{\xi} = 0$ in a finite time $T < \infty$ or it never hits this hyperplane. Thus, the global exponential stability of (59)–(63) and consequently that of the original closed-loop system (1), (14), (15), (58) is guaranteed whenever $\gamma_0 = 0$. This completes the proof of Theorem 4. □

Remark 4: In contrast to the state feedback design (cf. Remark 2), the observer-based controller (58) is only robust against vanishing disturbances because the observer model (14) and (15) is only capable of tracking the state of the system up to a certain estimation error, which decreases as the disturbance magnitude decreases.

Remark 5: As in the state feedback design (cf. Remark 3), the output feedback controller (58) with $\gamma_0 = 0$ is continuous at the origin, thereby eliminating around the equilibrium solution undesired high-frequency state oscillations caused by fast switching in the control signal.

In analogy to the state feedback design, the implementation of the discontinuous output feedback (63) can be performed through its continuous version

$$u(y, \tilde{\xi}, \tilde{x}_2) = -[\gamma_0 + \gamma_1 \|\tilde{\xi}\| + \gamma_2 \|y - C_1 M^{-1} \tilde{\xi} - C_2 \tilde{x}_2\|] B_{12}^{-1} \frac{\sigma\tilde{\xi}}{\|\sigma\tilde{\xi}\| + \delta^3}. \tag{81}$$

As opposed to the discontinuous feedback (63), its continuous approximation (81) does not excite undesirable high frequency state oscillations, whereas the resulting closed-loop system is practically stabilized in the following sense.

Theorem 5: *Let system* (1) *and observer* (14) *and* (15) *be enforced by a continuous approximation* (81) *of the discontinuous dynamic output feedback* (63) *subject to* (23) *and* (57). *Then, given initial conditions* $x(0) = x^0$, $\tilde{x}_1(0) = \tilde{x}_1^0$, $\tilde{x}_2(0) = \tilde{x}_2^0$ *and sufficiently small* $\delta > 0$, *the closed-loop system* (1), (14), (15) *and* (63) *has a unique solution* $x^\delta(t), \tilde{x}_1^\delta(t), \tilde{x}_2^\delta(t)$, *which is globally defined for all* $t \geq 0$. *Moreover, this system is Lyapunov stable, and for arbitrary* $\epsilon > 0$ *there exist* $\delta_0(\epsilon) > 0$ *and* $T_0(x^0, \tilde{x}_1^0, \tilde{x}_2^0, \epsilon) > 0$ *such that*

$$\|x^\delta(t)\|, \|\tilde{x}_1^\delta(t)\|, \|\tilde{x}_2^\delta(t)\| < \epsilon \quad \text{for all} \quad t \geq T_0(x^0, \tilde{x}_1^0, \tilde{x}_2^0, \epsilon) \text{ and } \delta \in (0, \delta_0). \tag{82}$$

Proof: The proof is similar to that of Theorem 3 and it is therefore omitted.

4. Numerical results

In this section, we present applications of the discontinuous output feedback controller design to the linearization of the one-dimensional KSE around its spatially-uniform steady state. The KSE describes incipient instabilities in a variety of physical and chemical systems and a control problem that occurs here is to avoid the appearance of the instabilities in the closed-loop system (Armaou and Christofides 2000). In order to smooth the response of the system the sliding mode-based controller is approximated by its continuous δ-counterparts, equation (52) in the state feedback case and (81) in the output feedback case. The objectives of the numerical simulations are to illustrate that: (1) the proposed δ-sliding-mode distributed output feedback controller is able to practically stabilize the linearized KSE at the spatially-uniform steady state solution with good robustness with respect to significant uncertainty in the instability parameter, ν, and (2) in the presence of non-vanishing external disturbance, the proposed δ-sliding-mode controller is superior to a linear feedback controller in terms of closed-loop performance. The two points are demonstrated in §4.1 and 4.2, respectively.

The linearized KSE with external disturbance is of the form

$$\frac{\partial x}{\partial t} = -\nu\frac{\partial^4 x}{\partial z^4} - \frac{\partial^2 x}{\partial z^2} + \sum_{i=1}^{m} b_i u_i(t) + d(z, t)$$
$$y_\kappa = \int_{-\pi}^{\pi} s_\kappa(z) x \,\mathrm{d}z, \ \kappa = 1, \ldots, p \tag{83}$$

subject to the periodic boundary conditions

$$\frac{\partial^j x}{\partial z^j}(-\pi, t) = \frac{\partial^j x}{\partial z^j}(+\pi, t), \quad j = 0, \ldots, 3 \tag{84}$$

and the initial condition

$$x(z, 0) = x_0(z) \tag{85}$$

where $x(z, t)$ is the state of the KSE, $z \in (-\pi, \pi)$ is the spatial coordinate, t is the time and 2π is the length of the spatial domain, ν is the instability parameter, and $x_0(z)$ is the initial condition. $u_i \in R$ denotes the ith manipulated input, m is the total number of manipulated inputs, $b_i(z) \in L_2(-\pi, \pi)$ is a square integrable function that represents the distribution function of the ith control actuator, p is the total number of measurement sensors, $y_\kappa \in R$ denotes a measured output, $s_\kappa(z) \in L_2(-\pi, \pi)$ is a square integrable function of z which is determined by the location and type of the measurement sensors, and $d(z, t)$ is an unknown uniformly bounded external disturbance to be rejected.

To simplify the presentation of our numerical results, we formulate (83)–(85) as an infinite-dimensional system in the Hilbert space of odd functions with spatial zero mean in the interval $(-\pi, \pi)$. This requires that the initial condition $x_0(z)$, the actuator distribution functions $b_i(z)$, $i = 1, \ldots, m$, and the external disturbance $d(z, t)$ are odd functions in the spatial variable z (this assumption imposes certain practical constraints on the shape of the actuator distribution functions, which will be discussed below in §4.1). Under this assumption, we formulate (83)–(85) as an infinite-dimensional system in the Hilbert space $L_2^{\text{odd}}(-\pi, \pi)$. To this end, we introduce the operator

$$Ax = -\nu\frac{\partial^4 x}{\partial z^4} - \frac{\partial^2 x}{\partial z^2} \tag{86}$$

with the dense domain

$$\mathcal{D}(A) = \left\{ x \in L_2^{\text{odd}}(-\pi, \pi): \ \frac{\partial^4 x}{\partial z^4}(z) \in L_2^{\text{odd}}(-\pi, \pi) \right.$$
$$\left. \frac{\partial^j x}{\partial z^j}(-\pi) = \frac{\partial^j x}{\partial z^j}(+\pi), \ j = 0, \ldots, 3 \right\} \tag{87}$$

and the input and measured output operators

$$Bu = \sum_{i=1}^{l} b_i u_i, \qquad Cx = \int_{-\pi}^{\pi} \mathcal{S}(z) x(z) \,\mathrm{d}z \tag{88}$$

where $\mathcal{S}(z) = (s_1(z), \ldots, s_p(z))^{\mathrm{T}}$. Then, the system (83)–(85) can be written as

$$\dot{x} = Ax + Bu + d, \qquad x(0) = x_0$$
$$y = Cx. \tag{89}$$

in the Hilbert space $L_2^{\text{odd}}(-\pi, \pi)$ where the operators B: $R^m \to L_2^{\text{odd}}(-\pi, \pi)$ and $C : L_2^{\text{odd}}(-\pi, \pi) \to R^p$ are bounded, and A is an unbounded operator (Pazy 1983).

In order to decompose the system (89) according to (10) and (11) into stable and unstable parts we formulate the following eigenvalue problem for A

$$A\phi_n = -\nu\frac{\partial^4 \phi_n}{\partial z^4} - \frac{\partial^2 \phi_n}{\partial z^2} = \lambda_n \phi_n, \ \ n = 1, \ldots, \infty \tag{90}$$

subject to

$$\frac{\partial^j \phi_n}{\partial z^j}(-\pi) = \frac{\partial^j \phi_n}{\partial z^j}(+\pi), \quad j = 0, \ldots, 3 \tag{91}$$

where λ_n denotes an eigenvalue and ϕ_n denotes an odd eigenfunction. A direct computation of the solution of the above eigenvalue problem yields $\lambda_n = -\nu n^4 + n^2$ with odd eigenfunctions $\phi_n(z) = (1/\sqrt{\pi}) \sin(nz)$, $n = 1, \ldots, \infty$. The spectrum $\{\lambda_1, \lambda_2, \ldots,\}$ of A is defined as the set of all eigenvalues of A. We note that the fact that A has a real pure point spectrum is a result of the fact that the spatial differential operator of the linearization of KSE with periodic boundary conditions is self-adjoint and the problem is considered in a bounded domain.

From the expression of the eigenvalues, it follows that for a fixed value of $\nu > 0$ the number of unstable eigenvalues of A is finite and the distance between two consecutive eigenvalues (i.e. λ_n and λ_{n+1}) increases as n increases. From these properties of the eigenspectrum of A, it follows that A generates an analytic semigroup (Curtain and Zwart 1995, Temam 1988).

By expanding the solution of the system (83) in an infinite series in terms of the odd eigenfunctions of the operator (90), we obtain

$$x(z, t) = \sum_{n=1}^{\infty} \alpha_n(t) \phi_n(z) \tag{92}$$

where $\alpha_n(t)$ is time-varying coefficient and $\phi_n(z) = (1/\sqrt{\pi}) \sin(nz)$. Substituting the above expansion for the solution, $x(z, t)$, into the system and taking the inner product in $L_2^{\text{odd}}(-\pi, \pi)$ with the eigenfunction $\phi_n(z)$, the following infinite-dimensional system of ODEs is obtained

$$\left.\begin{aligned} \dot{\alpha}_n &= (-\nu n^4 + n^2)\alpha_n + \sum_{i=1}^{m} b_{\alpha i}^n u_i(t) \\ &\quad + d_\alpha^n(t), \quad n = 1, \ldots, \infty \\ y_\kappa &= \int_{-\pi}^{\pi} s_\kappa(z)\left(\sum_{n=1}^{\infty}\alpha_n(t)\phi_n(z)\right)\mathrm{d}z, \quad \kappa = 1, \ldots, p \end{aligned}\right\} \tag{93}$$

where

$$b_{\alpha i}^n = \int_{-\pi}^{\pi} b_i(z)\phi_n(z)\,\mathrm{d}z \tag{94}$$

and

$$d_\alpha^n(t) = \int_{-\pi}^{\pi} d(z,t)\phi_n(z)\,\mathrm{d}z. \tag{95}$$

All simulation runs were performed for $\nu = 0.2$, using a 30-order linear ordinary differential equation model obtained from the application of modal decomposition to the system (83) (the use of higher-order approximations led to identical numerical results, thereby implying that the following simulation runs are independent of the discretization).

4.1. *Application to the linearized KSE without external disturbance*

In this subsection, we demonstrate that the proposed sliding-mode distributed feedback controller is capable of stabilizing of the spatially-uniform steady state of the linearized KSE when there is no external disturbance (i.e. $d(z, t) \equiv 0$). We observe that the system (93) possesses two unstable eigenvalues, and thus for $\nu = 0.2$, the spatially uniform steady-state $x(z, t) = 0$ is unstable. Therefore, we consider the first two modes of the linearization of KSE as the slow modes and use modal decomposition to construct a second-order ODE system. Two actuators are used to guarantee the exponential stabilizability of the system. At this point, it is important to point out that our choice to consider the linearized KSE as an infinite-dimensional system in the Hilbert space of odd functions with spatial zero mean in order to simplify the presentation of the controller synthesis formulas imposes certain practical constraints on the shape of the actuator distribution functions; it requires, for example, that $b_i(z)$ are odd functions, e.g. $b_i(z) = \phi_i(z)$, $i = 1, 2$. While it is possible to proceed with a such choice for $b_i(z)$, from a practical point of view as well as to study the effect of the control action on the fast modes (not accounted in the model used for controller design, i.e. "spillover" effect), it is preferable to consider the use of point control actuators. Therefore, we assume that we have available for the control of the KSE two point control actuators, placed at $z_{a1} = 0.31\pi$ and $z_{a2} = 0.69\pi$ (Lou and Christofides 2003) with following actuator distribution functions:

$$b_i(z) = \begin{cases} \dfrac{1}{\varepsilon_b} & \text{if } z_{a_i} - \dfrac{\varepsilon_b}{2} < z < z_{a_i} + \dfrac{\varepsilon b}{2}, \\ 0 & \text{if otherwise} \end{cases} \quad i = 1, \ldots, m \tag{96}$$

where ε_b is a constant representing the width of control actuation in the spatial interval $(-\pi, \pi)$ (note that the above selection of $b_i(z)$ ensures that $b_i(z) \in L_2(-\pi, \pi)$). In this work, $\varepsilon_b = 0.1$ in all closed-loop simulations.

The second-order ODE system resulting from the application of modal decomposition to the linearized KSE is of the form

$$\begin{bmatrix} \dot{\alpha}_1 \\ \dot{\alpha}_2 \end{bmatrix} = \begin{bmatrix} \lambda_1 & 0 \\ 0 & \lambda_2 \end{bmatrix}\begin{bmatrix} \alpha_1 \\ \alpha_2 \end{bmatrix} + \begin{bmatrix} b_{\alpha 1}^1 & b_{\alpha 2}^1 \\ b_{\alpha 1}^2 & b_{\alpha 2}^2 \end{bmatrix}\begin{bmatrix} u_1 \\ u_2 \end{bmatrix} \tag{97}$$

where $b_{\alpha i}^n$ $(i, n = 1, 2)$ are computed by using (94).

The first simulation run was performed to evaluate the ability of the sliding-mode state feedback controller to stabilize the system (83). The continuous approximation of the sliding-mode state feedback controller (22), (52) takes the form

$$\begin{bmatrix} u_1 \\ u_2 \end{bmatrix} = -(\gamma_0 + \gamma_1\|\xi\|)B_{12}^{-1}\frac{\xi}{\|\xi\| + \delta_c^3} \tag{98}$$

where

$$\xi = \begin{bmatrix} b_{\alpha 1}^1 & b_{\alpha 2}^1 \\ b_{\alpha 1}^2 & b_{\alpha 2}^2 \end{bmatrix}^{\mathrm{T}}\begin{bmatrix} \alpha_1 \\ \alpha_2 \end{bmatrix} \quad \text{and}$$

$$B_{12} = \begin{bmatrix} b_{\alpha 1}^1 & b_{\alpha 2}^1 \\ b_{\alpha 1}^2 & b_{\alpha 2}^2 \end{bmatrix}^{\mathrm{T}}\begin{bmatrix} b_{\alpha 1}^1 & b_{\alpha 2}^1 \\ b_{\alpha 1}^2 & b_{\alpha 2}^2 \end{bmatrix}.$$

The controller parameters used in the simulation are $\gamma_0 = 5.0$, $\gamma_1 = 5.0$, and $\delta_c^3 = 0.005$.

The system is assumed to be at the initial condition:

$$x_0 = 1.35\sin(z) \in L_2^{\mathrm{odd}}(-\pi, \pi). \tag{99}$$

The closed-loop spatio-temporal profile of $x(z,t)$ and the profiles of the two manipulated inputs are shown in figure 2. It is clear that the controller stabilizes the state of the system at $x(z,t) = 0$.

The second simulation run was performed to evaluate the ability of the sliding-mode output feedback controller to stabilize the system (83). Two point measurement sensors are used in this simulation to guarantee the exponential detectability of the system. The measurement sensors are placed at $z_{s1} = 0.35\pi$ and $z_{s2} = 0.64\pi$ (Lou and Christofides 2003). Based on the two measurements, $[y_1\, y_2]^{\mathrm{T}}$, and the 30-order approximation of the infinite-dimensional system (93), the state observer is of the following form

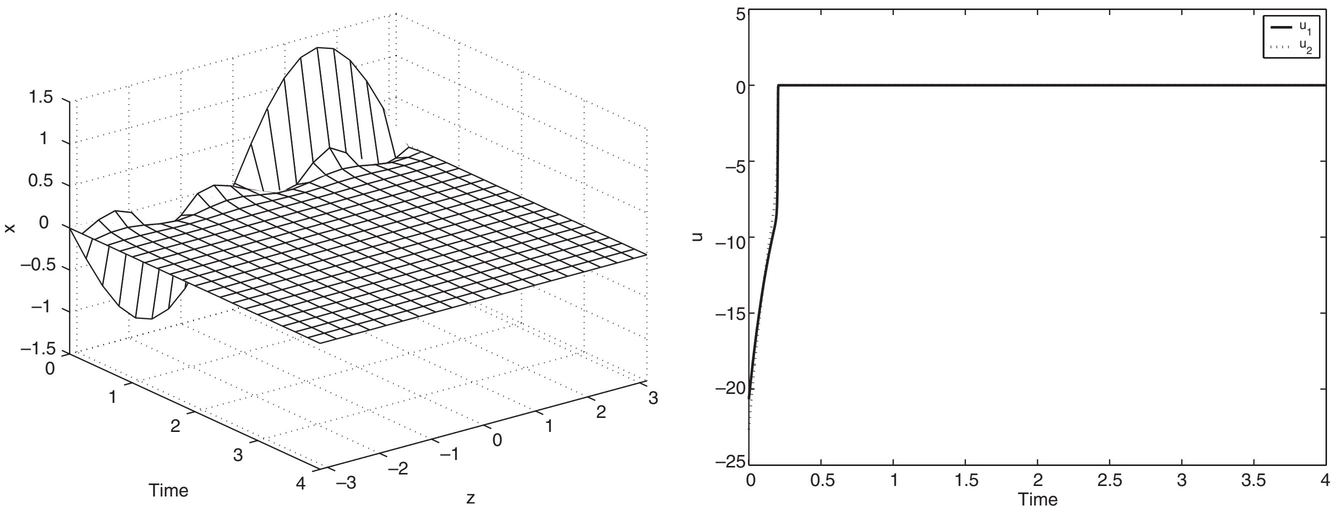

Figure 2. Closed-loop spatio-temporal profile of $x(z, t)$ (left figure) and manipulated input profiles (right figure) under δ-sliding-mode state feedback control.

$$\begin{bmatrix}\dot{\tilde{\alpha}}_1\\ \dot{\tilde{\alpha}}_2\end{bmatrix} = \begin{bmatrix}\lambda_1 & 0\\ 0 & \lambda_2\end{bmatrix}\begin{bmatrix}\tilde{\alpha}_1\\ \tilde{\alpha}_2\end{bmatrix} + \begin{bmatrix}b_{\alpha1}^1 & b_{\alpha2}^1\\ b_{\alpha1}^2 & b_{\alpha2}^2\end{bmatrix}\begin{bmatrix}u_1\\ u_2\end{bmatrix} - L_1\left(\begin{bmatrix}y_1\\ y_2\end{bmatrix} - C_1\begin{bmatrix}\tilde{\alpha}_1\\ \tilde{\alpha}_2\end{bmatrix} - C_2\begin{bmatrix}\tilde{\alpha}_3\\ \vdots\\ \tilde{\alpha}_{30}\end{bmatrix}\right)$$

$$\begin{bmatrix}\dot{\tilde{\alpha}}_3\\ \vdots\\ \dot{\tilde{\alpha}}_{30}\end{bmatrix} = \begin{bmatrix}\lambda_3 & \cdots & 0\\ \vdots & \ddots & \vdots\\ 0 & \cdots & \lambda_{30}\end{bmatrix}\begin{bmatrix}\tilde{\alpha}_3\\ \vdots\\ \tilde{\alpha}_{30}\end{bmatrix} + \begin{bmatrix}b_{\alpha1}^3 & b_{\alpha2}^3\\ \vdots & \vdots\\ b_{\alpha1}^{30} & b_{\alpha2}^{30}\end{bmatrix}\begin{bmatrix}u_1\\ u_2\end{bmatrix} \tag{100}$$

where

$$C_1 = \begin{bmatrix}c_1^1 & c_1^2\\ c_2^1 & c_2^2\end{bmatrix} \tag{101}$$

$$C_2 = \begin{bmatrix}c_1^3 & \cdots & c_1^{30}\\ c_2^3 & \cdots & c_2^{30}\end{bmatrix} \tag{102}$$

c_κ^n is given by

$$c_\kappa^n = \int_{-\pi}^{\pi} s_\kappa(z)\phi_n(z)\,\mathrm{d}z \tag{103}$$

the function $s_\kappa(z)$ is of the form

$$s_\kappa(z) = \begin{cases}\dfrac{1}{\varepsilon_s} & \text{if} \quad z_{s_\kappa} - \dfrac{\varepsilon_s}{2} < z < z_{s_\kappa} + \dfrac{\varepsilon_s}{2}\\ 0 & \text{if} \quad \text{otherwise}\end{cases}, \quad \kappa = 1, \ldots, p. \tag{104}$$

z_{s_κ} is the location of the κth measurement sensor and ε_s is a constant representing the width of the distributed sensing in the spatial interval $(-\pi, \pi)$. In this work, $\varepsilon_s = 0.1$ in all closed-loop simulations.

L_1 is set to be

$$L_1 = -10\begin{bmatrix}c_1^1 & c_1^2\\ c_2^1 & c_2^2\end{bmatrix}^{-1} \tag{105}$$

The observer outputs are used to compute the control action via the following continuous sliding-mode controller (based on (63) and (81))

$$\begin{bmatrix}u_1\\ u_2\end{bmatrix} = -\left(\gamma_0 + \gamma_1\left\|\tilde{\xi}\right\| + \gamma_2\left\|\tilde{\zeta}\right\|\right)B_{12}^{-1}\frac{\tilde{\xi}}{\left\|\tilde{\xi}\right\| + \delta_c^3} \tag{106}$$

where

$$\tilde{\xi} = \begin{bmatrix}b_{\alpha1}^1 & b_{\alpha2}^1\\ b_{\alpha1}^2 & b_{\alpha2}^2\end{bmatrix}^{\mathrm{T}}\begin{bmatrix}\tilde{\alpha}_1\\ \tilde{\alpha}_2\end{bmatrix},$$

$$\tilde{\zeta} = \begin{bmatrix}y_1\\ y_2\end{bmatrix} - C_1\begin{bmatrix}\tilde{\alpha}_1\\ \tilde{\alpha}_2\end{bmatrix} - C_2\begin{bmatrix}\tilde{\alpha}_3\\ \vdots\\ \tilde{\alpha}_{30}\end{bmatrix}$$

and

$$B_{12} = \begin{bmatrix}b_{\alpha1}^1 & b_{\alpha2}^1\\ b_{\alpha1}^2 & b_{\alpha2}^2\end{bmatrix}^{\mathrm{T}}\begin{bmatrix}b_{\alpha1}^1 & b_{\alpha2}^1\\ b_{\alpha1}^2 & b_{\alpha2}^2\end{bmatrix}.$$

The following values are used for the parameters of the controller of $\gamma_0 = 5.0$, $\gamma_1 = 5.0$, $\gamma_2 = 5.0$, and $\delta_c^3 = 0.005$.

The initial condition for the system is the same to that in (99) and the initial condition for the state observer is given as

$$\tilde{x}_0 = 1.0\sin(z) + \frac{0.1}{\sqrt{\pi}}\sum_{n=2}^{30}\sin(nz) \in L_2^{\mathrm{odd}}(-\pi, \pi). \tag{107}$$

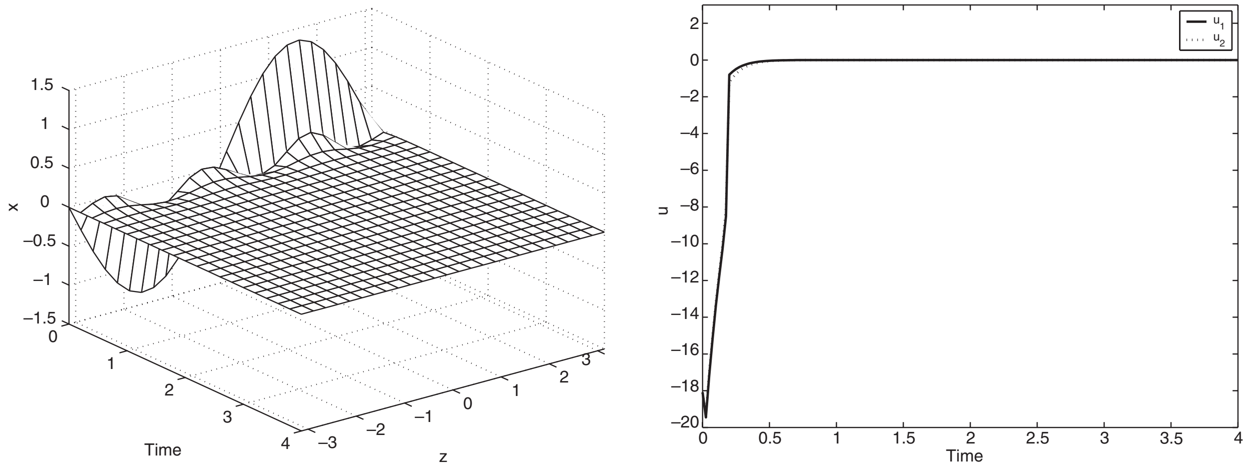

Figure 3. Closed-loop spatio-temporal profile of $x(z, t)$ (left figure) and manipulated input profiles (right figure) under δ-sliding-mode output feedback control.

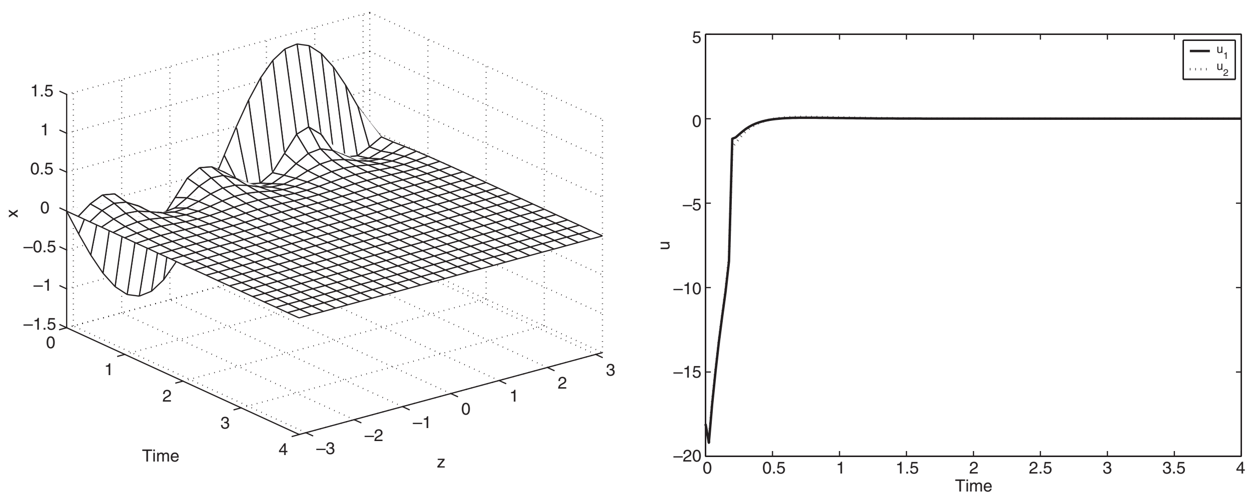

Figure 4. Closed-loop spatio-temporal profile of $x(z, t)$ (left figure) and manipulated input profiles (right figure) under δ-sliding-mode output feedback control for 25% uncertainty in ν.

The closed-loop spatio-temporal profile of $x(z, t)$ and the profiles of the two manipulated inputs are shown in figure 3. It is clear that the proposed sliding-mode output feedback controller stabilizes the state of the system at $x(z, t) = 0$.

The third simulation run was performed to test the robustness of the output feedback control law (100)–(106), for a 25% decrease in the value of the instability parameter (i.e. ν was taken to be equal to 0.15 in the high-order discretization of the linearization of KSE but it was used as 0.2 in the controller and state observer); this corresponds to a vanishing disturbance since, $x(z, t) = 0$, for the uncertain system, continues to be an equilibrium solution. Figure 4 shows the closed-loop spatio-temporal profile of the state and profiles of the two manipulated inputs, using initial conditions for the system and for the state observer same to those in (99) and (107), respectively. Our simulation clearly shows that the proposed sliding-mode output feedback controller is capable of stabilizing the linearized KSE at the spatially-uniform steady state solution in the presence of significant uncertainty in ν.

4.2. *Application to the linearized KSE with non-vanishing external disturbance*

In this subsection, we demonstrate that in the presence of external non-vanishing disturbance, the proposed sliding-mode feedback controller is superior to a linear feedback controller in terms of closed-loop performance. All the simulation runs shown in this subsection were performed for $\nu = 0.2$, using a 30-order linear ordinary differential equation model obtained from the application of modal decomposition to the system (83) (the use of higher-order approximations led to identical numerical results, thereby implying that the following simulation runs are independent of the discretization). We consider the first five modes of the linearization of KSE as the slow modes and use

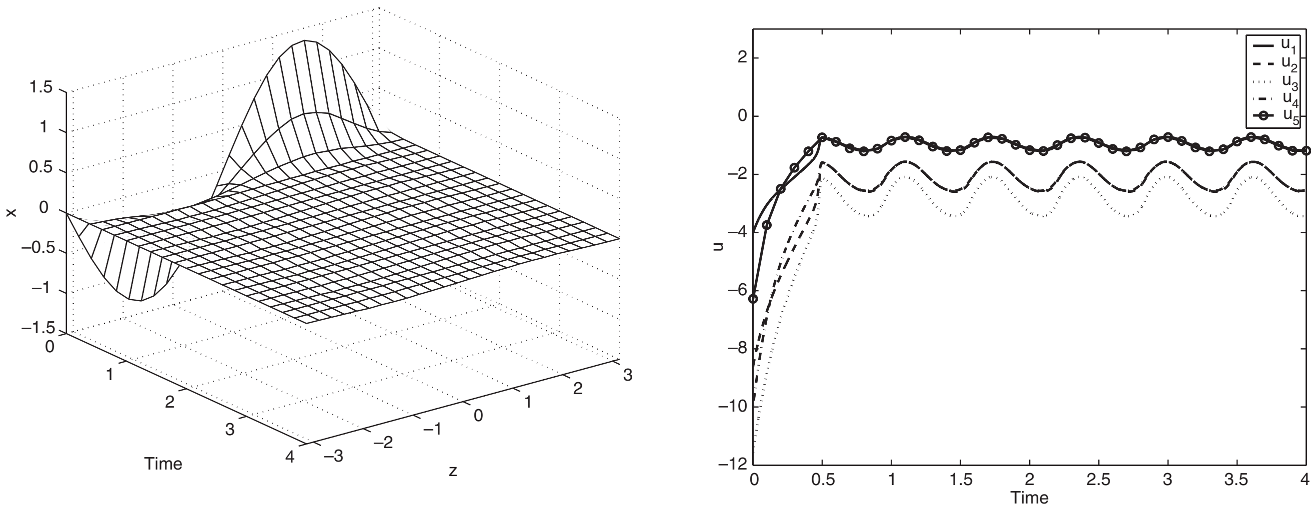

Figure 5. Closed-loop spatio-temporal profile of $x(z, t)$ (left figure) and manipulated input profiles (right figure) under δ-sliding-mode state feedback control with external disturbance ($d(z, t) = (1/\sqrt{\pi})\sin(z)[4 + \sin(10t)]$).

modal decomposition to construct a fifth-order ODE system. Five actuators are used to control the system. The resulting fifth-order ODE system is of the form

$$\begin{bmatrix} \dot{\alpha}_1 \\ \vdots \\ \dot{\alpha}_5 \end{bmatrix} = \begin{bmatrix} \lambda_1 & \dots & 0 \\ \vdots & \ddots & \vdots \\ 0 & \dots & \lambda_5 \end{bmatrix} \begin{bmatrix} \alpha_1 \\ \vdots \\ \alpha_5 \end{bmatrix} + \begin{bmatrix} b^1_{\alpha 1} & \cdots & b^1_{\alpha 5} \\ \vdots & \ddots & \vdots \\ b^5_{\alpha 1} & \cdots & b^5_{\alpha 5} \end{bmatrix} \begin{bmatrix} u_1 \\ \vdots \\ u_5 \end{bmatrix} + \begin{bmatrix} d^1_{\alpha} \\ \vdots \\ d^5_{\alpha} \end{bmatrix} \tag{108}$$

where $b^n_{\alpha i}$ $(i, n = 1, \dots, 5)$ are computed by using (94) with the actuator distribution functions, $b_i(z)$, of the form as shown in (96) and d^i_{α} $(i = 1, \dots, 5)$ are computed by using (95) with $d(z, t)$ of the form

$$d(z, t) = \frac{1}{\sqrt{\pi}}\sin(z)[4 + \sin(10t)]. \tag{109}$$

The first simulation run was performed to compare the closed-loop performance under the sliding-mode state feedback control and that under linear state feedback control in the presence of non-vanishing external disturbance (109). For the system (108), the continuous approximation (52) of the discontinuous sliding-mode state feedback controller (22) takes the form:

$$\begin{bmatrix} u_1 \\ \vdots \\ u_5 \end{bmatrix} = -(\gamma_0 + \gamma_1\|\xi_d\|)B_d^{-1}\frac{\xi_d}{\|\xi_d\| + \delta_c^3} \tag{110}$$

where

$$\xi_d = \begin{bmatrix} b^1_{\alpha 1} & \dots & b^1_{\alpha 5} \\ \vdots & \ddots & \vdots \\ b^5_{\alpha 1} & \cdots & b^5_{\alpha 5} \end{bmatrix}^{\mathrm{T}} \begin{bmatrix} \alpha_1 \\ \vdots \\ \alpha_5 \end{bmatrix}$$

and

$$B_d = \begin{bmatrix} b^1_{\alpha 1} & \cdots & b^1_{\alpha 5} \\ \vdots & \ddots & \vdots \\ b^5_{\alpha 1} & \dots & b^5_{\alpha 5} \end{bmatrix}^{\mathrm{T}} \begin{bmatrix} b^1_{\alpha 1} & \dots & b^1_{\alpha 5} \\ \vdots & \ddots & \vdots \\ b^5_{\alpha 1} & \dots & b^5_{\alpha 5} \end{bmatrix}.$$

To reject the non-vanishing external disturbance, we assume that the upper bound of the external disturbance is known and the parameter γ_0 in (110) is larger than the upper bound of the external disturbance. The controller parameters used in this simulation are the same to those used in §4.1.

The linear state feedback controller is designed as

$$\begin{bmatrix} u_1 \\ \vdots \\ u_5 \end{bmatrix} = -k \begin{bmatrix} b^1_{\alpha 1} & \cdots & b^1_{\alpha 5} \\ \vdots & \ddots & \vdots \\ b^5_{\alpha 1} & \dots & b^5_{\alpha 5} \end{bmatrix}^{-1} \begin{bmatrix} \alpha_1 \\ \vdots \\ \alpha_5 \end{bmatrix} \tag{111}$$

where the gain value $k = 9.503$ is selected for the simulation.

To compare the closed-loop performance of the two controllers, we use a performance index of the following form:

$$J(t_f) = \int_0^{t_f}\int_{-\pi}^{\pi} x^2(z, t)\,\mathrm{d}z\,\mathrm{d}t \tag{112}$$

where $x(z, t)$ is the state of the closed-loop system and t_f is the total simulated time. Throughout, this time is set to $t_f = 4$.

The initial condition of the system is the same to (99) and the locations of the five actuators are $z_{a_1} = 0.15\pi$, $z_{a_2} = 0.31\pi$, $z_{a_3} = 0.5\pi$, $z_{a_4} = 0.69\pi$ and $z_{a_5} = 0.85\pi$.

Figure 5 shows the spatio-temporal profile of $x(z, t)$ and profiles of the five manipulated inputs under the sliding-mode state feedback controller (110). It is clear

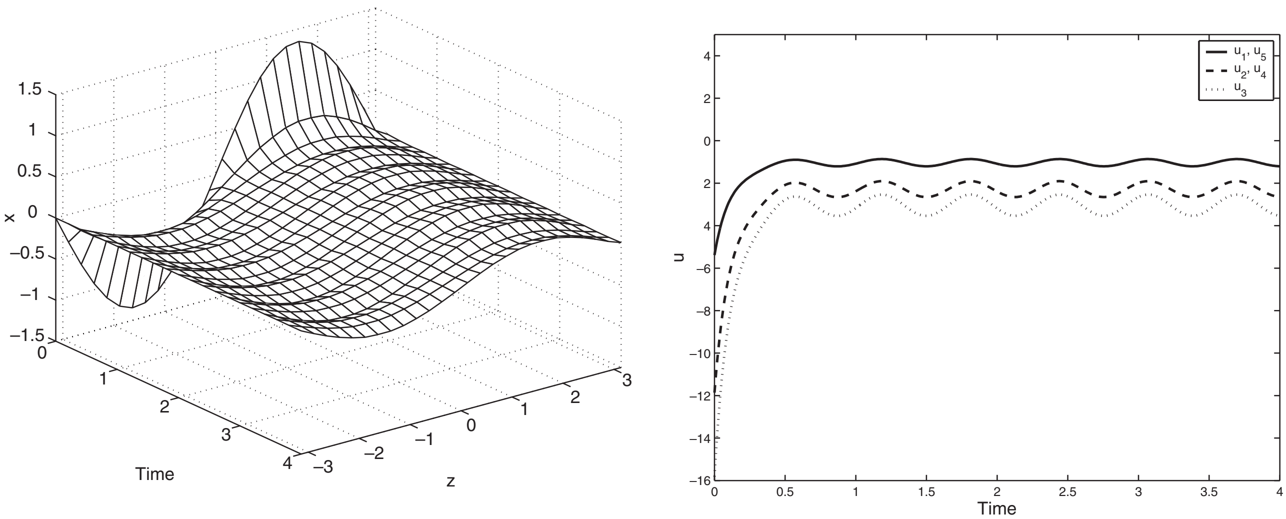

Figure 6. Closed-loop spatio-temporal profile of $x(z, t)$ (left figure) and manipulated input profiles (right figure) under linear state feedback control with external disturbance ($d(z, t) = (1/\sqrt{\pi})\sin(z)[4 + \sin(10t)]$).

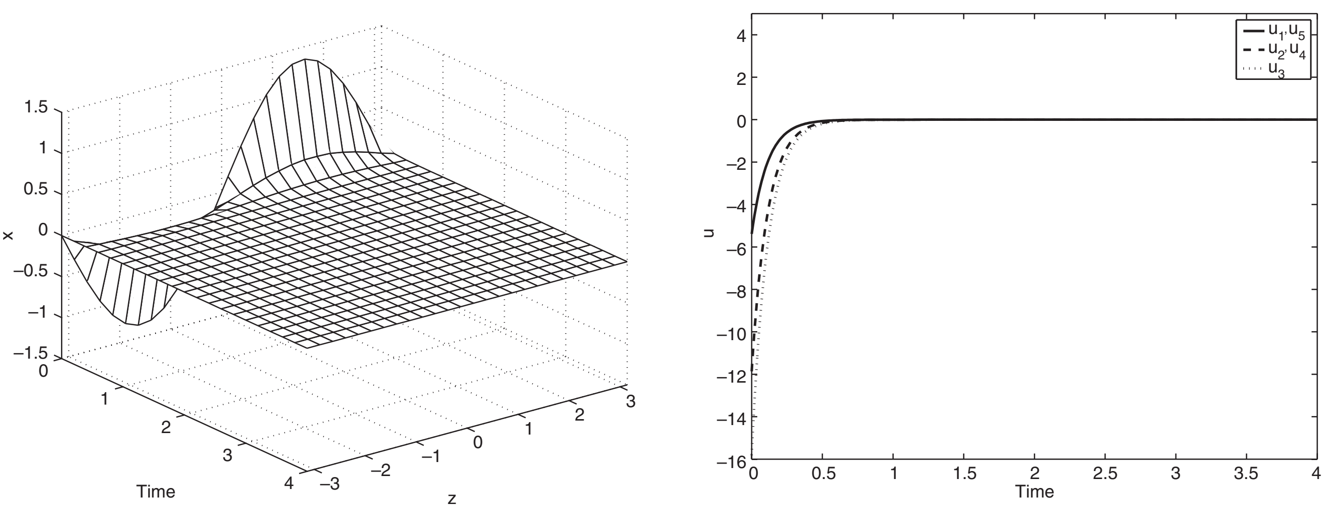

Figure 7. Closed-loop spatio-temporal profile of $x(z, t)$ (left figure) and manipulated input profiles (right figure) under linear state feedback control without external disturbance; $J(t_f) = \int_0^{t_f}\int_{-\pi}^{\pi} x^2(z, t)\,\mathrm{d}z\,\mathrm{d}t = 0.3567$.

that this controller is capable of stabilizing the state of the system as $x(z, t) = 0$ in the presence of non-vanishing external disturbance. The value of the performance index, corresponding to (110), is $J(t_f) = 0.5731$.

Figure 6 shows the spatio-temporal profile of $x(z, t)$ and profiles of the five manipulated inputs under linear state feedback control. We can see that the linear state feedback controller is not able to drive the state of the system to $x(z, t) = 0$ in the presence of non-vanishing external disturbance. Moreover, the value of the performance index is $J(t_f) = 1.3263$ which is much larger than that under the δ-sliding-mode state feedback controller (110).

Remark 6: We note that the superior closed-loop performance achieved by the proposed δ-sliding-mode feedback controller is not due to the poor tuning of the linear feedback controller. The gain k of the linear state feedback controller (111) is tuned such that the performance under this linear controller is the same to that under the δ-sliding-mode state feedback controller (110) with respect to the performance index defined in (112), when there is no external disturbance. Figures 7 and 8 show the closed-loop spatio-temporal profile of $x(z, t)$ and the profiles of the five manipulated inputs under the linear state feedback controller and the δ-sliding-mode state feedback controller without external disturbance. $J(t_f) = \int_0^{t_f}\int_{-\pi}^{\pi} x^2(z, t)\,\mathrm{d}z\,\mathrm{d}t = 0.3567$ in both cases. Comparing figures 7 and 8 to figures 6 and 5, we can see that while both controllers (110) and (111) can achieve the same performance without the presence of external disturbance, the closed-loop

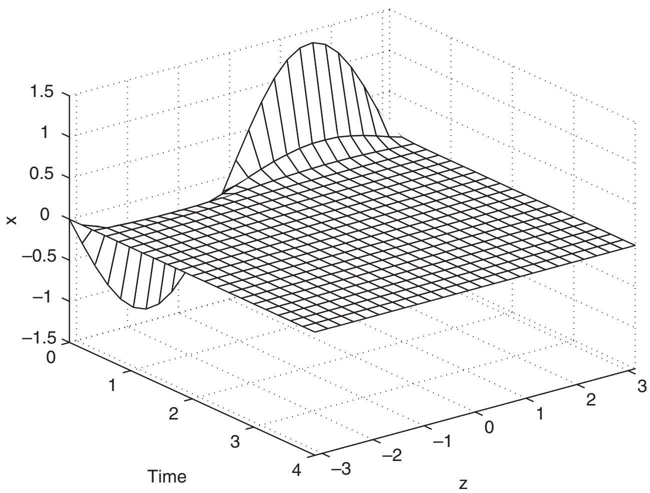

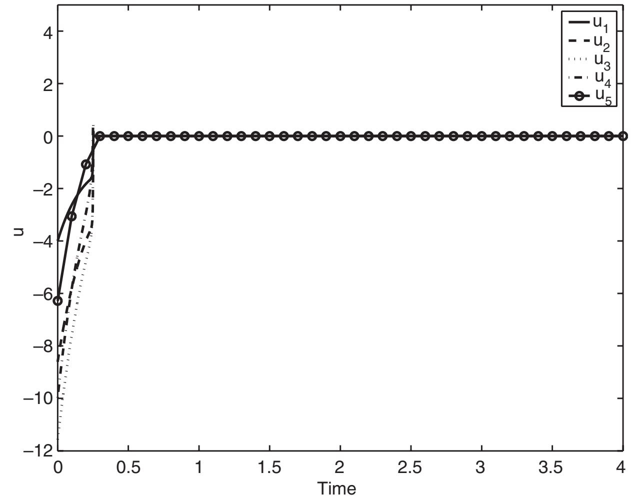

Figure 8. Closed-loop spatio-temporal profile of $x(z, t)$ (left figure) and manipulated input profiles (right figure) under δ-sliding-mode state feedback control without external disturbance; $J(t_f) = \int_0^{t_f}\int_{-\pi}^{\pi} x^2(z, t)\,\mathrm{d}z\,\mathrm{d}t = 0.3567$.

performance is significantly deteriorated by the non-vanishing disturbance under the linear state feedback control law (111) but it is not deteriorated under the δ-sliding-mode state feedback control law (110).

Finally, we compare the closed-loop performance under the sliding-mode output feedback controller and the linear output feedback controller in the presence of non-vanishing external disturbance. Two measurement sensors are used in this simulation. The sensors are placed at $z_{s1} = 0.35\pi$ and $z_{s2} = 0.64\pi$ (Lou and Christofides 2003). Based on the two measurements, $[y_1 \quad y_2]^{\mathrm{T}}$, and the 30-order approximation of the infinite-dimensional system (93), the state observer is of the form

$$\begin{bmatrix} \dot{\tilde{\alpha}}_1 \\ \vdots \\ \dot{\tilde{\alpha}}_5 \end{bmatrix} = \begin{bmatrix} \lambda_1 & \dots & 0 \\ \vdots & \ddots & \vdots \\ 0 & \dots & \lambda_5 \end{bmatrix} \begin{bmatrix} \tilde{\alpha}_1 \\ \vdots \\ \tilde{\alpha}_5 \end{bmatrix} + \begin{bmatrix} b^1_{\alpha 1} & \cdots & b^1_{\alpha 5} \\ \vdots & \ddots & \vdots \\ b^5_{\alpha 1} & \cdots & b^5_{\alpha 5} \end{bmatrix} \times \begin{bmatrix} u_1 \\ \vdots \\ u_5 \end{bmatrix} - L_{d1}\left(\begin{bmatrix} y_1 \\ y_2 \end{bmatrix} - C_{d1} \begin{bmatrix} \tilde{\alpha}_1 \\ \vdots \\ \tilde{\alpha}_5 \end{bmatrix} - C_{d2} \begin{bmatrix} \tilde{\alpha}_6 \\ \vdots \\ \tilde{\alpha}_{30} \end{bmatrix} \right)$$

$$\begin{bmatrix} \dot{\tilde{\alpha}}_6 \\ \vdots \\ \dot{\tilde{\alpha}}_{30} \end{bmatrix} = \begin{bmatrix} \lambda_6 & \cdots & 0 \\ \vdots & \ddots & \vdots \\ 0 & \cdots & \lambda_{30} \end{bmatrix} \begin{bmatrix} \tilde{\alpha}_6 \\ \vdots \\ \tilde{\alpha}_{30} \end{bmatrix} + \begin{bmatrix} b^6_{\alpha 1} & \cdots & b^6_{\alpha 5} \\ \vdots & \ddots & \vdots \\ b^{30}_{\alpha 1} & \cdots & b^{30}_{\alpha 5} \end{bmatrix} \begin{bmatrix} u_1 \\ \vdots \\ u_5 \end{bmatrix}$$

where

$$C_{d1} = \begin{bmatrix} c^1_1 & \cdots & c^5_1 \\ c^1_2 & \cdots & c^5_2 \end{bmatrix} \tag{114}$$

$$C_{d2} = \begin{bmatrix} c^6_1 & \cdots & c^{30}_1 \\ c^6_2 & \cdots & c^{30}_2 \end{bmatrix} \tag{115}$$

c^n_κ ($\kappa = 1, 2$ and $n = 1, \dots, 30$) is given by (103). L_{d1} is set to be

$$L_{d1} = \begin{bmatrix} -61.503 & -45.274 & 11.395 & 52.714 & 47.944 \\ -64.149 & 44.218 & 17.044 & -56.905 & 42.524 \end{bmatrix}^{\mathrm{T}} \tag{116}$$

The state estimates of (113) are used in the following δ-sliding-mode controller

$$\begin{bmatrix} u_1 \\ \vdots \\ u_5 \end{bmatrix} = -\left(\gamma_0 + \gamma_1 \left\|\tilde{\xi}_d\right\| + \gamma_2 \left\|\tilde{\zeta}_d\right\|\right) B_d^{-1} \frac{\tilde{\xi}_d}{\left\|\tilde{\xi}_d\right\| + \delta^3_c} \tag{117}$$

where

$$\tilde{\xi}_d = \begin{bmatrix} b^1_{\alpha 1} & \cdots & b^1_{\alpha 5} \\ \vdots & \ddots & \vdots \\ b^5_{\alpha 1} & \cdots & b^5_{\alpha 5} \end{bmatrix}^{\mathrm{T}} \begin{bmatrix} \tilde{\alpha}_1 \\ \vdots \\ \tilde{\alpha}_5 \end{bmatrix},$$

$$\tilde{\zeta} = \begin{bmatrix} y_1 \\ y_2 \end{bmatrix} - C_{d1} \begin{bmatrix} \tilde{\alpha}_1 \\ \vdots \\ \tilde{\alpha}_5 \end{bmatrix} - C_{d2} \begin{bmatrix} \tilde{\alpha}_6 \\ \vdots \\ \vdots \\ \tilde{\alpha}_{30} \end{bmatrix}$$

and

$$B_d = \begin{bmatrix} b^1_{\alpha 1} & \dots & b^1_{\alpha 5} \\ \vdots & \ddots & \vdots \\ b^5_{\alpha 1} & \cdots & b^5_{\alpha 5} \end{bmatrix}^{\mathrm{T}} \begin{bmatrix} b^1_{\alpha 1} & \cdots & b^1_{\alpha 5} \\ \vdots & \ddots & \vdots \\ b^5_{\alpha 1} & \cdots & b^5_{\alpha 5} \end{bmatrix}.$$

The values of γ_0, γ_1, γ_2 and δ^3_c are the same to those used in § 4.1.

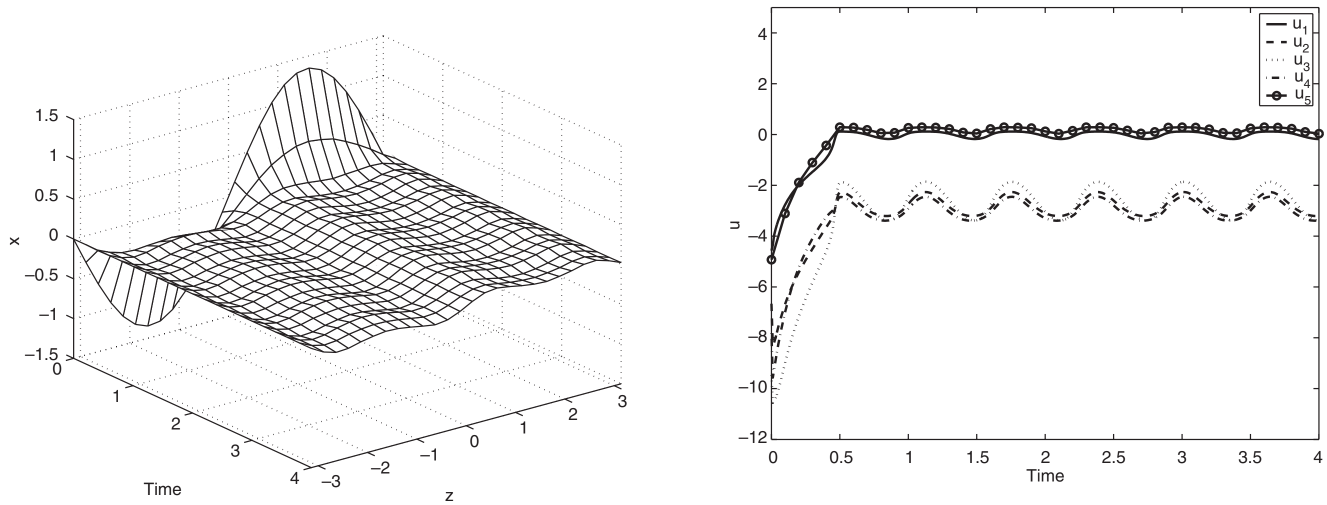

Figure 9. Closed-loop spatio-temporal profile of $x(z, t)$ (left figure) and manipulated input profiles (right figure) under δ-sliding-mode output feedback control with external disturbance ($d(z, t) = (1/\sqrt{\pi})\sin(z)[4 + \sin(10t)]$).

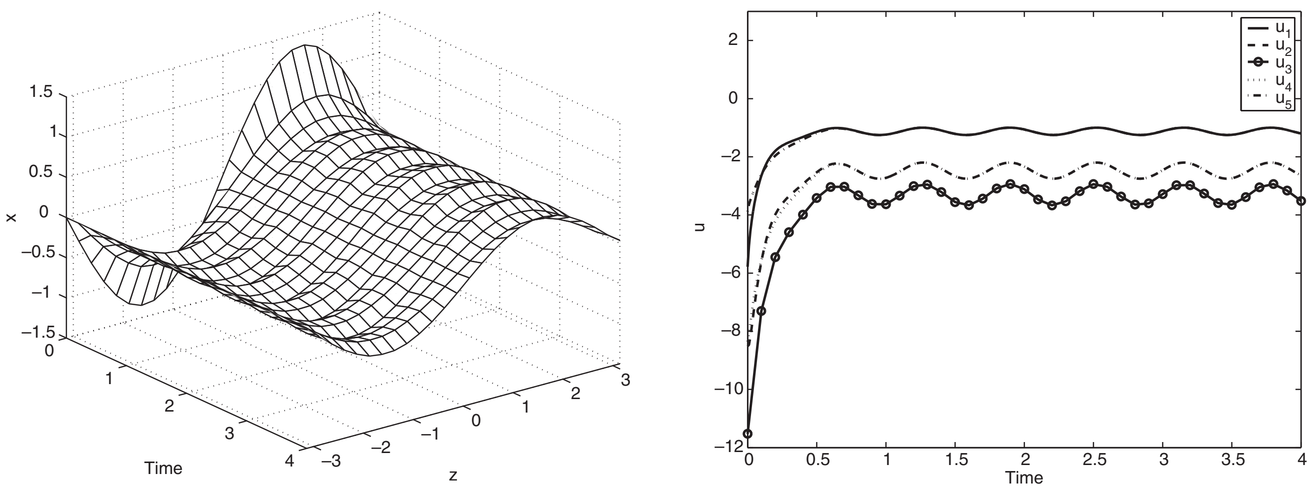

Figure 10. Closed-loop spatio-temporal profile of $x(z, t)$ (left figure) and manipulated input profiles (right figure) under linear output feedback control with external disturbance ($d(z, t) = (1/\sqrt{\pi})\sin(z)[4 + \sin(10t)]$).

In turn, the state estimates (113) are also used in the linear controller

$$\begin{bmatrix} u_1 \\ \vdots \\ u_5 \end{bmatrix} = -k \begin{bmatrix} b^1_{\alpha 1} & \cdots & b^1_{\alpha 5} \\ \vdots & \ddots & \vdots \\ b^5_{\alpha 1} & \dots & b^5_{\alpha 5} \end{bmatrix}^{-1} \begin{bmatrix} \tilde{\alpha}_1 \\ \vdots \\ \tilde{\alpha}_5 \end{bmatrix} \quad (118)$$

where the gain value $k = 9.503$ is the same as before.

Using as initial condition for the system the same to that in (99) and initial condition for the state observer the same to that in (107), the closed-loop spatio-temporal profile of $x(z, t)$ and the profiles of the five manipulated inputs under sliding-mode output feedback controller (113)–(117) are shown in figure 9. We can clearly see that the δ-sliding-mode output feedback controller (113)–(117) is able to efficiently suppress the influence of the non-vanishing external disturbance to the state of the system and drive the state of the system very close to $x(z, t) = 0$ achieving, at the same time, very good performance (performance index $J(t_f) = 0.7522$). Figure 10 shows the closed-loop spatio-temporal profile of $x(z, t)$ and the profiles of the five manipulated inputs under the linear output feedback controller (113)–(116) and (118). The performance index under the linear output feedback control law is $J(t_f) = 4.0886$, which is much larger than that under the δ−sliding-mode output feedback controller.

Remark 7: We note that it is important to implement the designed state/output feedback sliding-mode controllers [(22) and (58)] by using their continuous approximations so that fast switching in the control actions can be avoided. To demonstrate the presence of fast switching in discontinuous sliding-mode controllers, we run

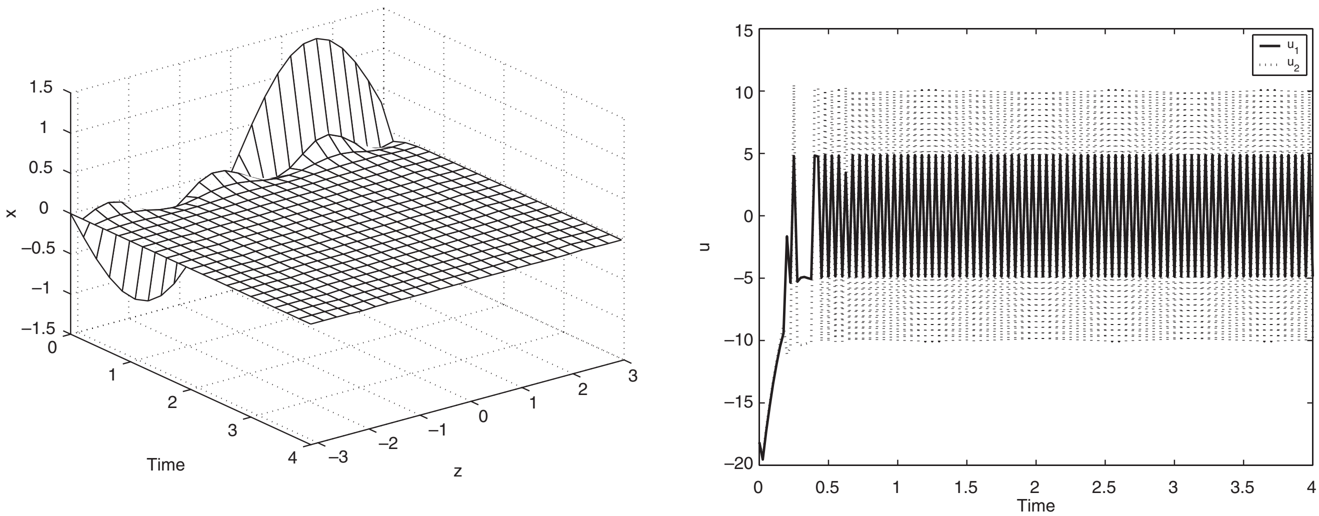

Figure 11. Closed-loop spatio-temporal profile of $x(z, t)$ (left figure) and manipulated input profiles (right figure) under sliding-mode output feedback control.

a simulation to stabilize the system (83) using the discontinuous output feedback sliding-mode controller of (63). The design of the output feedback controller and the state observer follows the development in (100)–(107) except that the δ_c^3 term is removed from the denominator of the controller. In figure 11, we show the closed-loop spatio-temporal profile of $x(z, t)$ and the profiles of the two manipulated inputs. Comparing figure 11 and figure 3, we can see that the closed-loop profiles of x from both simulations are very close, but the manipulated inputs from the δ-sliding-mode output feedback controller are much smoother than those from the discontinuous sliding-mode output feedback controller. Therefore, the δ-sliding-mode controllers are preferable from a practical implementation point of view.

5. Conclusions

Sliding-mode controllers have been widely used in practice due to simplicity of their implementation and strong robustness properties against unmodelled dynamics and parameter variations. In the infinite-dimensional setting the sliding mode-based synthesis has only been developed under the restrictive assumption that distributed sensing over the entire spatial domain is available. In the present paper, a fully practical framework is proposed for the synthesis of sliding-mode output feedback controllers for linear infinite-dimensional systems with finite-dimensional unstable part when finite-dimensional sensing and actuation are only available. The proposed framework involves a finite-dimensional approximation of the infinite-dimensional Luenberger observer and a continuous approximation of the sliding-mode controller. Although the case of bounded control and observation operators is only studied, the extension to unbounded point actuators and sensors seems possible. The proposed control method was used to stabilize the linearization of the Kuramoto–Sivashinsky equation around the spatially-uniform steady state solution in the presence of vanishing and non-vanishing disturbances. The sliding-mode controller was found to be superior to a linear feedback controller in terms of closed-loop performance in the presence of non-vanishing disturbances.

References

Armaou, A., and Christofides, P. D., 2000, Wave suppression by nonlinear finite-dimensional control. *Chemical Engineering Science*, **55**: 2627–2640.

Christofides, P. D., 2001, *Nonlinear and Robust Control of PDE Systems: Methods and Applications to Transport-Reaction Processes* (Boston: Birkhäuser).

Christofides, P. D., and Armaou, A., 2000, Global stabilization of the Kuramoto–Sivashinsky equation via distributed output feedback control. *Systems and Control Letters*, **39**: 283–294.

Curtain, R. F., and Zwart, H. J., 1995, *An Introduction to Infinite-Dimensional Linear Systems Theory* (New York: Springer-Verlag).

Foias, C., Ozbay, H., and Tannenbaum, A., 1996, *Robust Control of Infinite Dimensional Systems: Frequency Domain Methods* (London: Springer-Verlag).

Ho, C. M., and Tai, Y. C., 1998, Micro-electro-mechanical-systems (MEMS) and fluid flows. *Annual Reviews of Fluid Mechanics*, **30**: 579–612.

Hu, C. B., and Temam, R., 2001, Robust control of the Kuramoto-Sivashinsky equation. *Dynamics of Continuous Discrete and Impulsive Systems - Series B - Applications and Algorithms*, **8**: 315–338.

Kobayashi, T., 2002, Adaptive stabilization of the Kuramoto-Sivashinsky equation. *International Journal of Systems Science*, **33**: 175–180.

Levaggi, L., 2002a, Infinite dimensional systems sliding motions. *European Journal of Control*, **8**: 508–518.

Levaggi, L., 2002b, Sliding modes in banach spaces. *Differential Integral Equations*, **15**: 167–189.

Liu, W.-J., and Krstic, M., 2001, Stability enhancement by boundary control in the Kuramoto-Sivashinsky equation. *Nonlinear Analysis: Theory, Methods and Applications*, **43**: 485–507.

Lou, Y., and Christofides, P. D., 2003, Optimal actuator/sensor placement for nonlinear control of the Kuramoto-Sivashinsky equation. *IEEE Transactions on Control Systems Technology*, **11**: 737–745.

Orlov, Y., 2000, Discontinuous unit feedback control of uncertain infinite-dimensional systems. *IEEE Transactions on Automatic Control*, **45**: 834–843.

Orlov, Y., and Dochain, D., 2002, Discontinuous feedback stabilization of minimum-phase semilinear infinite-dimensional systems with application to chemical tubular reactor. *IEEE Transactions on Automatic Control*, **47**: 1293–1304.

Orlov, Y., and Utkin, V. I., 1987, Sliding mode control in infinite-dimensional systems. *Automatica*, **23**: 753–757.

Pazy, A., 1983, *Semigroups of Linear Operators and Applications to Partial Differential Equations* (New York: Springer-Verlag).

Sussman, H. J., and Kokotovic, P. V., 1991, The peaking phenomenon and the global stabilization of nonlinear systems. *IEEE Transactions on Automatic Control*, **36**: 424–440.

Temam, R., 1988, *Infinite-Dimensional Dynamical Systems in Mechanics and Physics* (New York: Springer-Verlag).

Utkin, V. I., 1992, *Sliding Modes in Control Optimization* (Berlin: Springer-Verlag).

Utkin, V. I., Guldner, J., and Shi, J., 1999, *Sliding Modes in Electromechanical Systems* (London: Taylor and Francis).

van Keulen, B., 1993, H_∞*-Control for Distributed Parameter Systems: A State-Space Approach* (Boston: Birkhäuser).

Zolezzi, T., 1989, Variable structure control of semilinear evolution equations. *Partial Differential Equations and the Calculus of Variations, Essays in Honor of Ennio De Giorgi* Birkhäuser, Boston, vol. 2, pp. 997–1018.